Sources and budgets for CO and O_3 in the northeastern Pacific during the spring of 2001: Results from the PHOBEA-II Experiment

Lyatt Jaeglé,[1] Daniel A. Jaffe,[2] Heather U. Price,[2,3] Peter Weiss-Penzias,[2] Paul I. Palmer,[4] Mathew J. Evans,[4] Daniel J. Jacob,[4] and Isabelle Bey[5]

[1] Ground and airborne measurements of CO, ozone, and aerosols were obtained in the northeastern (NE) Pacific troposphere during 9 March–31 May 2001 as part of the PHOBEA-II project (Photochemical Ozone Budget of the Eastern North Pacific Atmosphere). The GEOS-CHEM global three-dimensional model of tropospheric chemistry was used for flight planning, as well as for data analysis after the field mission to examine the origin of CO and ozone over the NE Pacific. The model successfully reproduces the observed CO levels, their temporal variability, and vertical gradients, strongly suggesting a good understanding of the sources, transport and chemistry of CO in the NE Pacific. For ozone the model underestimates mean surface observations by 8 ppbv, overestimates aircraft profiles by 5 ppbv, and does not reproduce the temporal variability of the observations. Possible explanations for model error in the ozone simulation are discussed. We find a pervasive influence of Asian and European anthropogenic sources on the levels of CO in the NE Pacific troposphere. In the 0–6 km column over our surface site, Asian and European emissions account for 33% (42 ppbv) and 15% (21 ppbv) of CO, respectively. Asian and European emissions are responsible for smaller fractions of the 0–6 km ozone column, 12% (5 ppbv) and 5% (2 ppbv), respectively. The full influence of Asian emissions (including secondary ozone production by export of its precursors) approaches 16% of ozone. The model successfully captures three intercontinental transport events observed during the PHOBEA-II campaign: one at the surface and two in the free troposphere. While all three events were characterized by large CO enhancements (by 20–40 ppbv), only one case showed significant ozone enhancement (by 20 ppbv), induced by high-latitude transport of Asian pollution mixed in with stratospheric ozone.   *INDEX TERMS:* 0322 Atmospheric Composition and Structure: Constituent sources and sinks; 0340 Atmospheric Composition and Structure: Middle atmosphere—composition and chemistry; 0341 Atmospheric Composition and Structure: Middle atmosphere—constituent transport and chemistry (3334); *KEYWORDS:* long-range transport, CO and O_3, Pacific

1. Introduction

[2] Ozone and carbon monoxide play key roles in the troposphere. Tropospheric ozone controls the oxidizing power of the atmosphere. At the surface, it is a major pollutant, harmful to human health and vegetation. In the middle and upper troposphere, ozone is an important greenhouse gas. Ozone is transported to the troposphere from the stratosphere, and is also produced in the troposphere by the oxidation of CO, methane and nonmethane hydrocarbons (NMHC) in the presence of nitrogen oxides ($NO_x = NO + NO_2$) and hydrogen oxides ($HO_x = HO + HO_2$) [e.g., *World Meteorological Organization* (*WMO*), 1999].

[3] Carbon monoxide provides the primary OH sink in much of the troposphere. In addition, CO is a useful tracer of anthropogenic activities. The major sources of CO are fossil fuel combustion, biomass burning, biofuel burning, and oxidation of atmospheric CH_4 and of NMHCs [*Logan et al.*, 1981]. The lifetime of CO is in the range of weeks to months, while ozone has a shorter lifetime, ranging from days to weeks, depending upon the environment.

[4] Observations from the late 19th and early 20th century combined with models suggest that Northern Hemi-

[1]Department of Atmospheric Sciences, University of Washington, Seattle, Washington, USA.
[2]Interdisciplinary Arts and Sciences, University of Washington, Bothell, Washington, USA.
[3]Also at Department of Chemistry, University of Washington, Seattle, Washington, USA.
[4]Division of Engineering and Applied Sciences and Department of Earth and Planetary Sciences, Harvard University, Cambridge, Massachusetts, USA.
[5]Swiss Federal Institute of Technology, Lausanne, Switzerland.

sphere tropospheric ozone concentrations have increased by 25–50% since preindustrial times due to increasing anthropogenic NO$_x$, CO, CH$_4$, and NMHC emissions from fossil fuel combustion and biomass burning [*Prather and Ehhalt*, 2001, and references therein]. East Asia, in particular, is a region experiencing rising emissions due to rapid economic growth over the last few decades [*Akimoto and Narita*, 1994; *Elliott et al.*, 1997; *van Aardenne et al.*, 1999; *Streets and Waldhoff*, 2000]. As a result, ozone in the boundary layer and lower troposphere of East Asia has been increasing by about 2% per year [*Logan*, 1994; *Lee et al.*, 1998]. Continued increases in NO$_x$ and NMHC emissions, especially in developing regions of the world, may cause tropospheric O$_3$ to increase more dramatically through the 21st century [*Prather and Ehhalt*, 2001].

[5] Observations have shown that Asian emissions of gases and aerosols can be transported to North America in 6–8 days, under certain meteorological conditions [*Andreae et al.*, 1988; *Kritz et al.*, 1990; *Parrish et al.*, 1992; *Jaffe et al.*, 1999, 2001, 2003; *Husar et al.*, 2001; *McKendry et al.*, 2001; *Kotchenruther et al.*, 2001a; *Price et al.*, 2003; *Thulasiraman et al.*, 2002]. Enhanced mixing ratios of CO, peroxyacetyl nitrate (PAN), NMHCs, radon, industrial aerosols, and mineral aerosols have been identified in these airmasses coming from East Asia. However, not all of these airmasses with clear anthropogenic signatures are characterized by ozone enhancements [*Jaffe et al.*, 2003], suggesting loss of ozone during transport over oceans or reduced photolysis rates over emission areas (and thereby weak ozone production) due to high aerosol loading [*Dickerson et al.*, 1997; *Liao et al.*, 1999; *He and Carmichael*, 1999]. Identification of ozone enhancements from long-range transport of Asian emissions is further complicated by the possible mixing of anthropogenic emissions with stratospheric ozone [*Carmichael et al.*, 1998].

[6] Based on chemical transport model (CTM) calculations, current emissions from Europe and Asia contribute on average 4–7 ppbv O$_3$ at the surface in North America, relative to a total background of 25–55 ppbv [*Berntsen et al.*, 1999; *Jacob et al.*, 1999; *Yienger et al.*, 2000; *Wild and Akimoto*, 2001; *Fiore et al.*, 2002]. A future doubling of Asian emissions might increase surface ozone by another 4 ppbv over Western North America [*Berntsen et al.*, 1999]. Such an increase would offset the benefits from domestic reductions in anthropogenic emissions in the U.S. [*Jacob et al.*, 1999]. However, these estimates remain highly uncertain, and current understanding of intercontinental transport of Asian effluents and their effects on the global troposphere are limited by the lack of observations constraining the CTM calculations of Asian sources, transport and chemical transformation.

[7] During the spring of 2001 the TRACE-P (Transport and Chemical Evolution over the Pacific) [*Jacob et al.*, 2003] and ACE-Asia (Aerosol Characterization Experiment-Asia) [*Huebert et al.*, 2003] experiments were both operating in the western North Pacific region, where they sampled the gas and aerosol composition of the Asian outflow. Simultaneously, we made ground and airborne observations in the northeastern (NE) Pacific as part of the PHOBEA-II project (Photochemical Ozone Budget of the Eastern North Pacific Atmosphere). The main goal of the PHOBEA project is to understand the impact of upstream anthropogenic emissions on the NE Pacific troposphere [*Jaffe et al.*, 2001; *Kotchenruther et al.*, 2001a]. During these three missions, several CTMs [*Kiley et al.*, 2003] were used for flight planning to optimize the value of observations in constraining and evaluating CTM simulations of Asian sources, outflow and chemical evolution [*Jacob et al.*, 2003].

[8] In this paper we utilize the PHOBEA-II ground and airborne observations in the NE Pacific during the spring of 2001, along with the GEOS-CHEM global model of tropospheric chemistry [*Bey et al.*, 2001a] to understand the sources of atmospheric CO and O$_3$ in the NE Pacific. *Price et al.* [2003] give a detailed description of the results from the airborne component of PHOBEA-II. In parallel papers in this issue, the GEOS-CHEM model is used to interpret the TRACE-P observations in the western Pacific [*Liu et al.*, 2003; *Palmer et al.*, 2003; Evans et al., Emissions, transformations, and impact of Asian NO$_x$, to be submitted to *Journal of Geophysical Research*, 2003, hereinafter referred to as Evans et al., submitted manuscript, 2003]. Our focus in this paper is to evaluate the current effects of Asian and European outflow in the NE Pacific. In particular we wish to address the following questions: What are the sources and budgets for CO and O$_3$ in the NE Pacific? Can global model simulations quantitatively capture intercontinental transport events arriving in the NE Pacific?

2.   Observations and Model

[9] The PHOBEA-II mission combined surface observations at the Cheeka Peak Observatory (CPO, 48.3°N, 124.6°W, 480 m) on the western tip of Washington State and airborne profiles to 6 km altitude in the area immediately off the coast from CPO. During the first phase of the PHOBEA experiment, we used this site for observations during March–April 1997 and March–April 1998 [*Jaffe et al.*, 2001] and conducted airborne measurements off the coast in the spring of 1999 [*Kotchenruther et al.*, 2001a].

2.1.   Ground-Based Observations

[10] For this work we began ground-based measurements of CO, O$_3$, PM10 and PM2.5 at CPO on 9 March 2001. The experimental methods for CO and O$_3$ are identical to those given by *Jaffe et al.* [2001]. Briefly, CO was measured by a commercial gas filter correlation infrared instrument (Advanced Pollution Instruments model 300) modified for higher sensitivity. Calibration occurred once per day with a working standard referenced to a NIST standard reference material. An instrument zero is performed every 20 min by routing the airstream through a heated catalyst that oxidizes CO to CO$_2$. Ozone was measured using a standard UV absorption instrument (Dasibi AH1008) with temperature and pressure compensation. Calibration of the ozone instrument was performed using a standard O$_3$ calibrator (Columbia Scientific) immediately prior to the campaign and zero checks were performed daily.

2.2.   Vertical Profiles

[11] For the vertical profiles we used a twin-engine Beechcraft Duchess aircraft. Profiles were conducted on 12 days during spring 2001: 29 and 31 March; 1, 5, 8, 9, 11, 14, 25, and 27 April; and 1 and 6 May. All profiles were

obtained in the vicinity of CPO at $48.31 \pm 0.03°N$ latitude, $124.63 \pm 0.08°W$ longitude, and at altitudes between 0 and 6 km. The Duchess aircraft can carry the pilot plus one passenger and approximately 240 kg of instrumentation. Carbon monoxide and ozone, as well as NMHCs and aerosol scattering coefficient, were measured onboard the aircraft [*Price et al.*, 2003]. We collected whole air samples in stainless steel canisters for measurements of CO (by gas chromatography with a reduction gas analyzer detector). In situ measurements of O_3 were obtained with a new light-weight UV absorption instrument (2B Technologies) [*Bognar and Birks*, 1996]. We have extensively tested this new instrument against a standard UV instrument (Dasibi) as well as against an ECC ozonesonde on flights during summer 2001 [*Snow et al.*, 2003], demonstrating very close agreement. *Price et al.* [2003] give more details on the instrumentation, calibration procedures and flight patterns.

2.3. GEOS-CHEM Model

[12] Global simulations of O_3-NO_x-NMHC chemistry are conducted with the GEOS-CHEM global three-dimensional (3-D) model of tropospheric chemistry [*Bey et al.*, 2001a] driven by GEOS DAO (Data Assimilation Office) assimilated meteorological data [*Schubert et al.*, 1993]. The simulations presented here use GEOS-CHEM version 4.33 (http://www.as.harvard.edu/chemistry/trop/geos/) and two years (2000–2001) of GEOS-3 assimilated meteorological observations with a horizontal resolution of 2° latitude by 2.5° longitude and 46 vertical layers. Meteorological inputs are available with a 3- to 6-hour time resolution depending on the variable. The simulations are initialized on 1 February 2001 after a one-year spin-up with a $4° \times 5°$ horizontal resolution to speed up the calculations.

[13] The tropospheric O_3 simulation includes a detailed description of O_3-NO_x-NMHC chemistry (24 tracers, 120 species, and over 200 chemical reactions) [*Bey et al.*, 2001a]. Recent updates to the GEOS-CHEM model are described by *Martin et al.* [2003]. In particular, for the simulations presented in our study, we are using a reaction probability $\gamma_{N2O5} = 0.03$ for the heterogeneous reaction $N_2O_5 + H_2O \rightarrow 2 HNO_3$ on aerosols in the GEOS-CHEM model. Earlier versions of the GEOS-CHEM model used $\gamma_{N2O5} = 0.1$, following the recommendation of *Jacob* [2000]. This recommendation was based on laboratory measurements of N_2O_5 hydrolysis with H_2SO_4/H_2O aerosol particles under stratospheric conditions [*Sander et al.*, 2000, and references therein]. However, in the troposphere, sulfuric acid aerosols are much more dilute and often contain ammonia and nitrate. Laboratory measurements under tropospheric conditions for dilute sulfuric acid aerosols as well as liquid $(NH_4)_2SO_4$ and NH_4HSO_4 aerosols indicate generally lower γ_{N2O5} values, ranging between 0.01 and 0.05, with a significant dependence on temperature and relative humidity [e.g., *Hu and Abbatt*, 1997; *Hallquist et al.*, 2000; *Kane et al.*, 2001]. For soot, an upper limit of $\gamma_{N2O5} < 0.02$ is recommended by *Sander et al.* [2003]. Reaction probabilities >0.02 have been measured for aqueous NaCl aerosols [*Zetzsch and Behnke*, 1992; *George et al.*, 1994]. Lower uptake coefficient ($\gamma_{N2O5} < 3 \times 10^{-3}$) were measured for $NaNO_3$ aerosols [*Mentel et al.*, 1999], dry $(NH_4)_2SO_4$ aerosols [*Mozurkewich and Calvert*, 1988; *Hu and Abbatt*, 1997], and dry NaCl aerosols [*Sander et al.*,

2003]. We have thus adopted an intermediate value of $\gamma_{N2O5} = 0.03$ for all aerosols in the GEOS-CHEM model. This smaller γ_{N2O5} results in a longer NO_x lifetime and thus an average 10% increase for NO_x, 10% increase for OH, 3–5 ppbv increase for ozone and 8–10 ppbv decrease in CO relative to the case with $\gamma_{N2O5} = 0.1$, consistent with the results of *Dentener and Crutzen* [1993]. The intermediate γ_{N2O5} value that we have chosen reflects the average temperature and relative humidity of the troposphere, but is likely to be too high for warm and humid boundary layer conditions and too low for colder middle and upper tropospheric conditions. Evans et al. (submitted manuscript, 2003) include a more sophisticated scheme for calculating γ_{N2O5} based on local temperature and relative humidity.

[14] Stratosphere-troposphere exchange of ozone is simulated with the Synoz (synthetic ozone) scheme of *McLinden et al.* [2000], using a global cross-tropopause flux of 475 Tg O_3 yr^{-1}. We use a base anthropogenic emission inventory for 1985 as described by *Wang et al.* [1998], including NO_x emissions from the Global Emission Inventory Activity (GEIA) [*Benkovitz et al.*, 1996], nonmethane hydrocarbon emissions from *Piccot et al.* [1992], and CO emissions from B. N. Duncan et al. (Model study of the variability and trends of carbon monoxide (1988–1997): 1. Model formulation, evaluation, and sensitivity, submitted to *J. Geophys. Res.*, 2003, hereinafter referred to as Duncan et al., submitted reference, 2003) and *Yevich and Logan* [2003]. These emissions are scaled to 1998 following *Bey et al.* [2001a]. We use the seasonally varying climatological biomass burning CO emissions developed by *Duncan et al.* [2003]. Biomass burning emissions for other species are based on the CO emissions using the emission factors described by *Staudt et al.* [2003]. Analysis of satellite observations show that biomass burning emissions in southeast Asia and India were close to average during spring 2001 [*Heald et al.*, 2003], justifying the use of a climatological average. For CO, our anthropogenic emissions for Asia (10°S–60°N, 60°–150°E) are 257 Tg yr^{-1} (fossil fuel: 160 Tg yr^{-1}; biofuel: 97 Tg yr^{-1}), with an additional 119 Tg yr^{-1} from biomass burning.

[15] The GEOS-CHEM tropospheric chemistry model has been extensively evaluated and used to study ozone and its precursors over different regions of the globe [e.g., *Bey et al.*, 2001a, 2001b; *Liu et al.*, 2002; *Fiore et al.*, 2002; *Palmer et al.*, 2001; *Li et al.*, 2002a, 2002b; *Martin et al.*, 2002]. In particular, the model reproduces well the observed latitudinal and vertical composition of the Asian chemical outflow over the western Pacific, as well as its episodic export [*Bey et al.*, 2001b; *Liu et al.*, 2002, 2003; *Palmer et al.*, 2003; C. L. Heald et al., Transpacific satellite and aircraft observations of Asian pollution, submitted to *J. Geophys. Res.*, 2003, hereinafter referred to as Heald et al., submitted manuscript, 2003]. The present study builds on these previous evaluations and extends them to examine the fate of the Asian chemical outflow and its impact on the NE Pacific troposphere.

[16] To investigate the origin of CO and ozone in the model we conducted two sensitivity simulations based on the full chemistry ozone simulation: (1) a tagged CO simulation resolving source regions using archived monthly averaged OH concentrations; (2) a tagged ozone run using archived daily rates of ozone (actually odd-oxygen, which is

Table 1. Source Contributions to CO Over the Northeastern Pacific From the Tagged CO Simulation[a]

Source Regions[b]	Northeastern Pacific: 0–6 km Columns 35–60°N, 165°W–125°W	Cheeka Peak Observatory: 0–6 km Columns 48.3°N, 124.8°W	Cheeka Peak Observatory: 48.3°N, 124.8°W, 480 m
Fuel combustion[c]			
North America	1.5[a] (10%)	1.7[a] (11%)	25[e] (17%)
Europe	2.4 (15%)	2.3 (15%)	25 (17%)
Asia	4.1 (26%)	4.0 (26%)	36 (24%)
Others	0.3 (2%)	0.3 (1%)	2 (2%)
Biomass burning			
Asia	1.2 (7%)	1.1 (7%)	6.8 (4.6%)
Others	1.3 (8%)	1.3 (8%)	9.2 (6.4%)
Atmospheric production[d]	5.0 (32%)	5.0 (32%)	43 (29%)
Total	15.8 (100%)	15.7 (100%)	147 (100%)

[a]Values are mean tropospheric columns (in 10^{17} molecules/cm^2) below 6 km altitude for 9 March–31 May 2001 from the tagged-CO simulation. Percentages are indicated in parenthesis.

[b]Source regions are defined as follows: North America (24–88°N;142.5–47.5°W), Europe (36–88°N; 17.5°W–65°E), Asia (−12.5–88°N; 65–153°E).

[c]Fuel combustion includes fossil fuel and biofuel combustion.

[d]Atmospheric production includes CO production from the oxidation of methane, isoprene, monoterpenes, acetone, and methanol.

[e]In this last column, values are in mixing ratios (in ppbv) for the tagged-CO simulation sampled at the location of CPO for 9 March–31 May 2001 (Figure 2).

a conserved tracer: $O_x = O_3 + NO_2 + 2 \times NO_3 + HNO_3 + PAN + HNO_4 + 3 \times N_2O_5$) production rates and loss frequencies. For the tagged CO simulation [*Bey et al.*, 2001b; *Li et al.*, 2002a], we focus on four anthropogenic tracers, "North American FF CO," "Asian FF CO," "Asian BB CO," and "European FF CO" (specific geographical regions are defined in Table 1). Each of the "FF" (Fossil Fuel) tracers combines contributions from fossil fuel and biofuel sources, while the Asian "BB" (Biomass Burning) tracer refers to biomass burning sources. For all the results presented here the "Asian CO" tracer will refer to the sum of FF and BB Asian CO tracers. In addition to direct emissions of CO there is a large chemical source form the oxidation of methane and NMHCs, which we treat following the approach of Duncan et al. (submitted manuscript, 2003). Loss of CO by reaction with OH and production of CO by oxidation of CH$_4$ and biogenic VOCs (isoprene, methanol, monoterpenes, and acetone) are calculated using monthly mean OH concentrations from the GEOS-CHEM full chemistry simulation. Using these OH concentrations, we calculate a lifetime of 6.3 years for methylchloroform, consistent with current best estimate of 5.99 years by *Prinn et al.* [2001] from methylchoroform measurements. More details on the tagged CO simulations can be found in the work of *Palmer et al.* [2003]. The tagged ozone simulation [*Li et al.*, 2002a; *Liu et al.*, 2002] transports eight O$_x$ tracers from different regions. We will refer to these tagged O$_x$ tracers as "tagged O$_3$" tracers as ozone generally represents more than 95% of O$_x$. Results will be presented for ozone originating in the stratosphere, upper troposphere (400 hPa-tropopause), middle troposphere (700–400 hPa) and lower troposphere (700 hPa-surface). The lower troposphere is further subdivided into three separate continental tracers (Asian, European and North American, see Table 1 for geographical regions) and one tracer over the Pacific Ocean.

[17] The tagged ozone simulation gives information on the direct export of ozone produced in the lower troposphere over the continent of origin: "tagged Asian O$_3$" represents the ozone produced from ozone precursors (natural and anthropogenic) within the lower troposphere above Asia. Evaluating secondary production of ozone resulting from free tropospheric transport of ozone precursors from Asian is less straightforward. Our approach is to conduct a simulation with Asian anthropogenic sources turned off. The difference (*delta* O$_3$ = standard simulation − simulation without Asian sources) should reflect the combined effects of direct transport and secondary production. One caveat is that the nonlinearity of ozone production results in an overestimate of ozone production from natural sources close to the continent of origin, and thus an underestimate of Asian contribution. We will thus estimate a lower limit of the contribution from exported precursors by comparing "delta O$_3$" to the "tagged Asian O$_3$" tracer.

3. Use of Global Model Forecasting to Identify Flight Days

[18] Vertical profiles were made on 12 days between 29 March and 6 May 2001 in the area immediately off the coast from Cheeka Peak Observatory (section 2.2). Consistent with the goals of the PHOBEA experiment, we targeted days when long-range transport from sources on the Eurasian continent seemed likely. We also sought to sample clean marine airmasses. However, we endeavored to avoid days affected by recent emissions from the west coast of North America. A number of tools were used to identify such days. This includes the GEOS-CHEM forecast results driven by meteorological GEOS-3 forecasts from NASA Goddard (http://polar.gsfc.nasa.gov/operations/terra.php). We also used local meteorological data, results from the University of Washington's high resolution MM5 simulations (http://www.atmos.washington.edu/mm5rt/), satellite infrared and visible imagery, the TOMS aerosol index (http://jwocky.gsfc.nasa.gov/aerosols/today_aero.html) and forecast trajectories using NOAA's Hybrid Single-Particle Lagrangian Integrated Trajectory (HYSPLIT) model (http://www.arl.noaa.gov/ready/hysplit4.html).

[19] As an example of the use of the model forecasts, Figure 1 shows the GEOS-CHEM CO forecast for 13 April
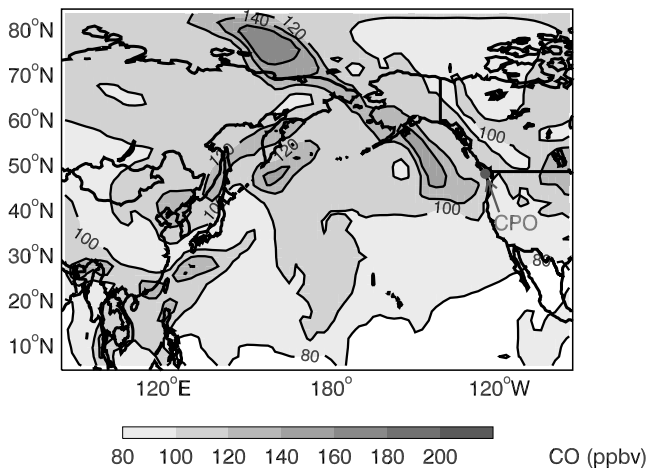
Figure 1. April 10 2001 (0 GMT) GEOS-CHEM model forecast for 13 April 2001 at 6 GMT. Total CO concentrations predicted at 600 hPa. The location of our measurement area at and above the Cheeka Peak Observatory (CPO: 48.3°N, 124.6°W) is indicated with a circle and arrow.

2001 at 6 GMT. This 3-day "look-ahead" forecast was initialized 0 GMT on 10 April. On 13 April, an airmass with a high mixing ratio of CO from Asia was predicted to be near the coast of Washington State. We conducted a vertical profile on 14 April 2001 between 1 and 2 GMT and indeed found significantly enhanced CO, aerosols and NMHCs at 4–6 km altitude [*Price et al.*, 2003]. In fact the CO and NMHC mixing ratios and the aerosol scattering coefficient in this airmass were the largest we observed during the spring of 2001. This airmass appears to have started as a large dust storm that originated in central Asia in early April and left the Asian continent on 8 April after picking up substantial amounts of anthropogenic emissions as it crossed East Asia. The dust storm was detected by the TOMS satellite Aerosol Index (AI) product and the Sea-WIFS sensors as it moved across the Pacific [*Price et al.*, 2003; *Thulasiraman et al.*, 2002; *Huebert et al.*, 2003].

4. Comparison of Model and Observations

4.1. Carbon Monoxide

[20] Figure 2 shows the observed CO mixing ratios at the CPO ground-site along with the GEOS-CHEM modeled values between 9 March and 31 May 2001. Both observations and model results (sampled at the location of CPO) are averaged over 4 hours. Model uncertainty (due to coarse horizontal resolution and errors in the meteorological fields) is assessed by also sampling the model in the grid boxes directly to the north, south, and west of CPO. The resulting range of mixing ratios is indicated with the gray shading on the upper panel of Figure 2. The model generally captures the observed levels, the slow decline of CO throughout April and May resulting from increasing levels of OH radical, as well as the timing and magnitude of periods with enhanced and low concentrations. The events with high levels of CO correspond to extended periods of easterly winds bringing air recently influenced by North American emissions (20 March, 15 April, 20 May). These conditions generally occur when a surface high pressure

system moves inland over the Pacific Northwest, resulting in low-level off-shore flow.

[21] Two notable exceptions to the good agreement are 4 April (model overpredicts observations by 40 ppbv) and 13–16 May (model underpredicts observations by 50 ppbv), which are characterized by a poor performance of the coarse 2° × 2.5° resolution wind fields in capturing sharp gradients in meteorological conditions near CPO. For example, on 4 April a pressure trough located over western Washington resulted in a sharp shift of surface winds from south westerly to northeasterly. The model placed CPO on the eastern side of the trough, influenced by North American emissions, while the CPO wind observations show that the site was still under southwesterly wind conditions. Indeed, when we sample the model in the grid box to the west of CPO we find much better agreement for this day (lower boundary of shaded gray area on Figure 2).

[22] Overall, there is very good agreement between modeled CO (146 ± 21 ppbv) and observed CO (150 ± 17 ppbv) for the time period of observations (Figure 4a). The correlation coefficient (r = 0.79) indicates that the model captures 62% of the day-to-day variability in CO. The spring 2001 CO observations are similar to 1997 observations (159 ppbv) but much lower than the observa-
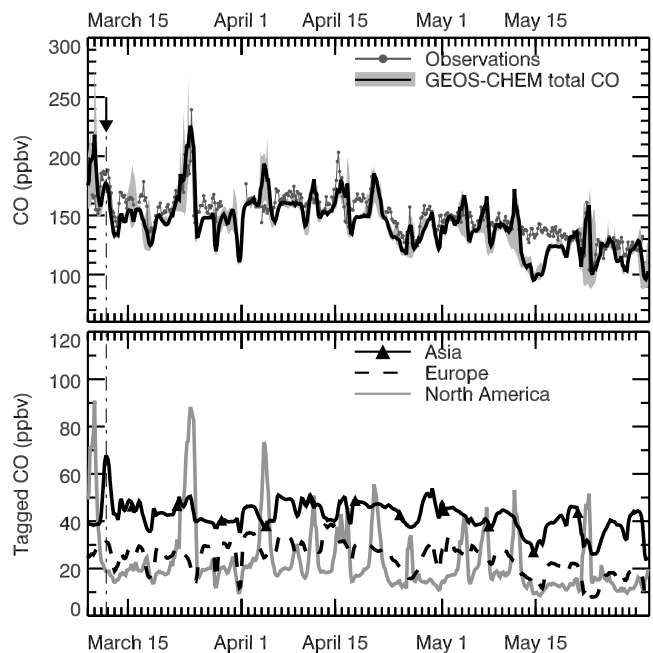

Figure 2. (top) 9 March–31 May 2001 comparison between model (black line) and observations (dark gray line with circles) at CPO for CO. Both model and observations are 4-hour averages. The GEOS-CHEM model is sampled at the location and altitude of CPO. Model uncertainty due to meteorology and resolution is assessed by also sampling grid boxes immediately to the north, west, and south of CPO. The gray shading indicates the resulting envelope of model results. (bottom) Time series of individual modeled contributions from Asian (solid line with triangles), North American (gray line), and European (dashed line) source regions at CPO. The arrow indicates the 11 March long-range transport event discussed in section 7.
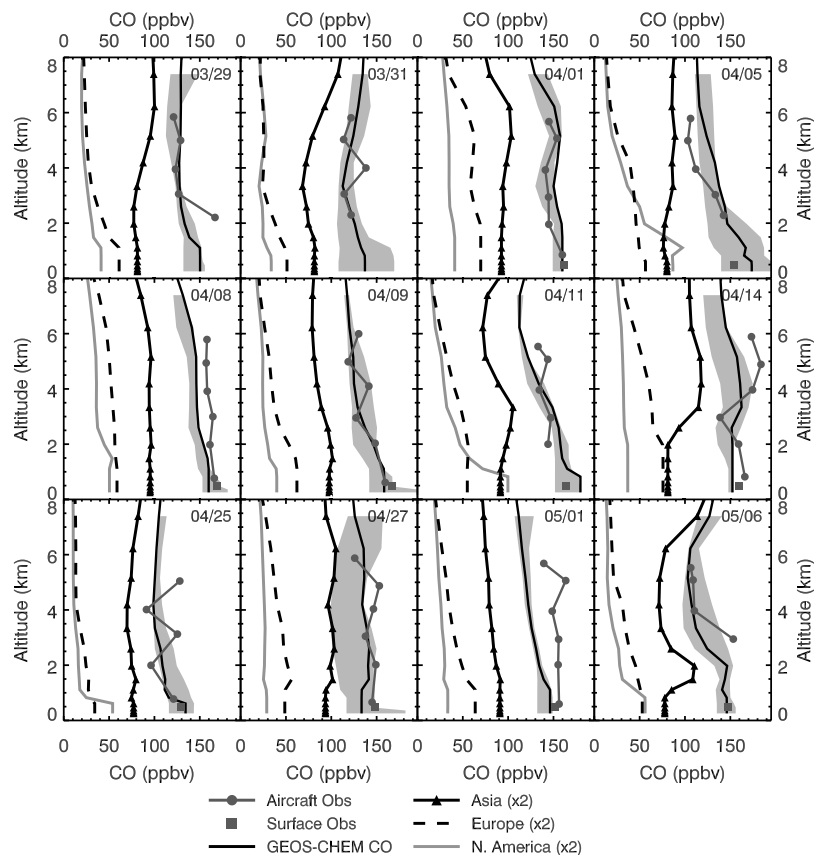
Figure 3.   Profiles of CO observed during the 12 flights of the Duchess aircraft between 29 March and 6 May 2001. The observations (dark gray circles connected by gray lines) are compared to results from the GEOS-CHEM model (black lines) sampled at the time and location of the observations. The gray square symbols indicate simultaneous observations of CO at the ground. Model uncertainty due to meteorology and resolution is assessed by also sampling grid boxes immediately to the north, west, south, and east of CPO within 6 hours of flight time. The light gray shading indicates the envelope of model results. Individual contributions from Asian, North American, and European source regions are also shown. Note that the individual contributions have been scaled by a factor of two for clarity.

tions in 1998 (177 ppbv) at CPO. *Jaffe et al.* [1999] attribute the higher values in 1998 to unusually high biomass burning emissions in Indonesia and Siberia.

[23] Figure 3 shows a comparison of observed and modeled CO mixing ratios as seen in the vertical profiles. One difficulty in this comparison is the short timescale (∼1 hour) and small spatial extent of the Duchess flights relative to the longer timescale on which wind fields are updated (6 hours) and the coarse horizontal resolution of the model. Given the variability in hourly CO levels (Figure 2), a small temporal and geographical displacement of meteorological features in the assimilated wind fields might lead to large discrepancies between modeled and observed profiles. To assess this potential error, we plot the modeled profile sampled at the time and location of the flights, and an envelope of four other profiles displaced in time by ±6 hours and displaced horizontally by one grid-box around CPO (gray shading in Figure 3). For most of the flights, there is little variability in the modeled profiles, reflecting the spatial uniformity of the modeled CO fields. However, in a few cases, such as 31 March and 5, 14, and 27 April, there are larger differences. The first 2 days correspond to periods of easterly low-levels winds bringing increasing

amounts of North American CO to the region, while the last 2 days reflect the arrival of Asian CO plumes in the free troposphere above the CPO site (see Figure 11).

[24] For the vertical profiles, the mean measured CO mixing ratio was 139 ± 20 ppbv, compared to a mean modeled value for the ensemble of flights of 136 ± 17 ppbv, showing very good agreement (Figure 4b). The correlation coefficient (r = 0.73) reflects the model's ability to capture the observed variability. The 2001 airborne profiles of CO show no statistically significant difference relative to the 1999 observations [*Price et al.*, 2003].

[25] We need to assess whether our sampling strategy (section 3) resulted in a dataset representative of all types of airmasses and chemical conditions characteristic of springtime NE Pacific troposphere. We thus compare in Figure 5 CO column densities up to 6 km above CPO, both for the observations and the GEOS-CHEM model. The observed column densities are obtained by combining aircraft profiles with the simultaneous ground-based CO observations at CPO. For the first two flights (29 March and 31 March), ground-based observations are not available and we use instead the 15 March–15 April observed mean value of 160 ppbv. The GEOS-CHEM CO columns
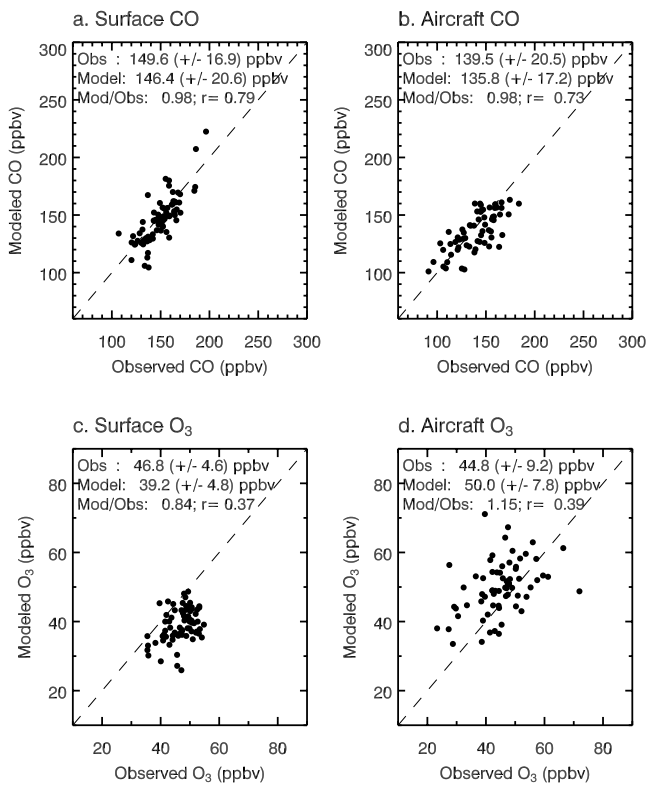
a. Surface CO
Obs : 149.6 (+/- 16.9) ppbv
Model: 146.4 (+/- 20.6) ppbv
Mod/Obs: 0.98; r= 0.79

b. Aircraft CO
Obs : 139.5 (+/- 20.5) ppbv
Model: 135.8 (+/- 17.2) ppbv
Mod/Obs: 0.98; r= 0.73

c. Surface O₃
Obs : 46.8 (+/- 4.6) ppbv
Model: 39.2 (+/- 4.8) ppbv
Mod/Obs: 0.84; r= 0.37

d. Aircraft O₃
Obs : 44.8 (+/- 9.2) ppbv
Model: 50.0 (+/- 7.8) ppbv
Mod/Obs: 1.15; r= 0.39

Figure 4. Scatter plot of daily averaged observed concentrations and modeled concentrations of CO and O_3 for the CPO ground site (a and c), and aircraft profiles (b and d) during spring 2001. The mean mixing ratios (±standard deviations) of the measured and modeled values are indicated in each panel, as well as the mean ratio between model and observations and the correlation coefficient (r). A line with a 1:1 slope is indicated with a dashed line.

were obtained at the location of CPO. For the days when measurements were made, the average 0–6 km CO column was 15.3×10^{17} molecules/cm^2 from the data and 14.6×10^{17} molecules/cm^2 from the GEOS-CHEM model sampled at the time closest to observations, showing good agreement. The mean modeled column for the 9 March–31 May period is 15.7×10^{17} molecules/cm^2. The similarity of the modeled column for all dates and the column for just the flight days suggests that the flight days are a good representation of CO levels for the entire time period. Furthermore, the relative importance among CO sources (33% Asia; 17% North America; 15% Europe, see Figure 5) is nearly identical for the model sampled for all flight dates and for the entire measurement time-period, implying that the choice of flights was representative of the mixture of sources influencing the NE Pacific.

[26] Heald et al. (submitted manuscript, 2003) (using the same GEOS-CHEM model version and emission inventory as this study, with the exception of a daily varying biomass burning inventory in Asia) have compared the full-year GEOS-CHEM model results for 2001 to NOAA/CMDL ground station CO measurements at representative sites in the Northern Hemisphere and find no bias in the simulation for spring. A comparison to satellite observations of CO columns from the MOPITT instrument during spring 2001

also shows no significant bias and a high correlation (Heald et al., submitted manuscript, 2003). The ability of the model in reproducing both background values and day-to-day variability in CO observations was also reported by Li et al. [2002a] in their comparisons of the GEOS-CHEM model to surface observations in the Atlantic at Sable Island and Mace Head. The level of agreement for CO is similar for both studies (Li et al.: r = 0.59–0.71, Mean Model/Obs = 0.88–0.94; this study at the CPO ground site, r = 0.79, Mean Model/Obs = 0.98). The very good agreement between model and observations for CO strongly suggests that the GEOS-CHEM model is accurately simulating the emission sources, transport, and CO chemistry. In contrast, comparisons between CO observations obtained in the Eastern Pacific during TRACE-P and chemical transport models show a significant negative bias of the models [*Kiley et al.*, 2003]. All the models in the intercomparison used the detailed CO fossil fuel and biofuel emission inventory developed by *Streets et al.* [2003] for Asia in 2000 (212 Tg yr^{-1}), which is 20% lower than our emission inventory (257 Tg yr^{-1}). *Palmer et al.* [2003] conducted an inverse modeling analysis using the TRACE-P CO observations and the GEOS-CHEM model driven by the Asian emission inventories from *Streets et al.* [2003] and Heald et al. (submitted manuscript, 2003). They find that a 30% increase in anthropogenic emissions over China, close to the levels used in our study, largely eliminates the model bias. *Streets et al.* [2003] and *Carmichael et al.* [2003] attribute the underprediction of Chinese emissions in their studies to an underreporting of domestic coal use in central China.

4.2. Ozone

[27] Figure 6 shows a comparison of measured and modeled O_3 at CPO, and Figure 7 shows a comparison for the twelve vertical profiles. At the ground, the model systematically underestimates the observations by 8 ppbv
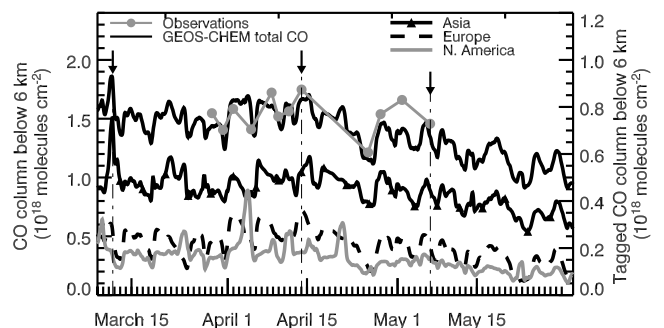

Figure 5. Timeseries of column CO concentrations at CPO (below 6 km altitude) between 9 March and 31 May 2001. The gray circles represent the observations on the twelve flight days, where surface levels of CO are taken from the ground-based observations. The solid black line shows the hourly GEOS-CHEM column. Also shown are the individual anthropogenic contributions from Asia (black line and triangles), North America (gray line), and Europe (dashed line) from the tagged CO simulation. Note the factor of two difference in scale for the total CO columns (left axis) and individual tagged components (right axis). The arrows indicate three long-range transport events from Asia discussed in section 7.
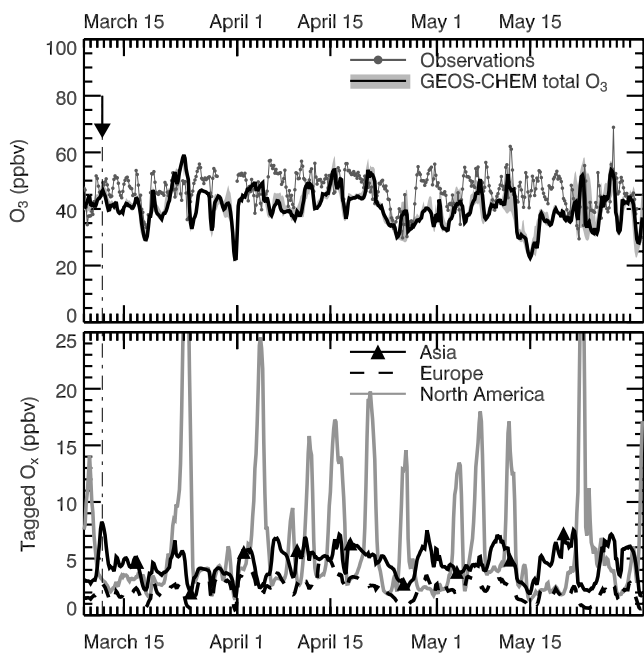
Figure 6. (top) 9 March–31 May 2001 comparison between 4-hour average model (black line) and observations (gray line with circles) at CPO for ozone. As in Figure 2, the envelope of model results of nearby gridboxes is indicated by the light gray shading. (bottom) Time series of individual modeled contributions from Asian, North American, and European source regions at Cheeka Peak from the tagged-O_x simulation. The arrow indicates the 11 March long-range transport event discussed in section 7.

(observations: 47 ± 5 ppbv; model: 39 ± 5 ppbv), while aloft the model overestimates the observations by 5 ppbv on average (observations: 45 ± 9 ppbv; model: 50 ± 8 ppbv) (Figures 4c and 4d). The model bias increases with increasing altitude. One possible explanation for the bias at CPO is related to heterogeneous loss of NO_x via N_2O_5 hydrolysis. As noted in section 2.3, *Hallquist et al.* [2000] and *Kane et al.* [2001] found a strong temperature and relative humidity dependence for γ_{N2O5}. Thus our use of a uniform $\gamma_{N2O5} = 0.03$ will tend to be too high in the boundary layer and too low in the colder middle and upper troposphere. A sensitivity simulation using $\gamma_{N2O5} = 0.1$ (more appropriate for the middle troposphere) decreases modeled ozone levels by 5 ppbv, nearly eliminating the positive bias in the free troposphere, while worsening the negative bias at the surface. Evans et al. (submitted manuscript, 2003) also find that their GEOS-CHEM modeling results over the western Pacific are very sensitive to assumptions about γ_{N2O5}. Using $\gamma_{N2O5} = 0.1$ in the model yields a systematic negative bias of 10 ppbv for O_3 compared to TRACE-P observations, and a factor of 2 overestimate of the observed boundary layer NO_x. On the other hand, assuming $\gamma_{N2O5} = 0.01$ largely resolves the O_3 negative bias and NO_x positive bias. Alternative explanations for the model bias include uncertainties in NO_x emission inventories, or a misrepresentation of stratospheric-tropospheric ozone flux for the time-period of observations.

[28] The weak correlation coefficient between model and observations (r < 0.4) reflects in part the small variability of observed ozone. We note that in their comparison of the GEOS-CHEM model to four Atlantic surface O_3 sites, *Li et al.* [2002a, 2002b] find a better correlation (r = 0.5–0.82), relative to our study (r = 0.37). One of the differences between the records compared is the large day-to-day variability in O_3 at the Atlantic sites presented by Li et al. (ozone background of 30–40 ppbv with levels ranging from 10 ppbv to 60 ppbv) driven by the proximity to source regions (Eastern north America for Sable Island and Bermuda; Europe for Mace Head and Westman Island). At Cheeka Peak Observatory in spring, the variability in observed ozone is weaker (background of 45 ppbv with two events up to 60 ppbv and two events down to 30 ppbv, Figure 6), reflecting the prevailing westerly winds bringing aged Pacific air from a complex mixture of sources (section 6). In addition, even during easterly wind conditions observed ozone levels remain low because of the high latitudes and low levels of pollution in western North America during spring. In fact North American influence on ozone at CPO appears to be overestimated in the model (section 6).

[29] The springtime observations of ozone obtained at CPO in 2001 are very similar to mean observations from the 1997 and 1998 (1997: 43 ppbv, 1998: 45 ppbv), while the airborne ozone profiles in 2001 are on average 11 ppbv lower than the profiles obtained in 1999 [*Kotchenruther et al.*, 2001a]. *Price et al.* [2003], attribute the greater levels of ozone in 1999 to enhanced stratosphere-troposphere exchange and/or biomass burning.

5. Pathways for Long-Range Transport of CO and Ozone to the North Eastern Pacific

[30] The main meteorological features influencing springtime transport over the North Pacific are the Siberian anticyclone, the Aleutian low, and the Pacific high. Spring is a transition period between the East Asian winter monsoon circulation to the summer monsoon circulation (starting in May) during which the Siberian anticyclone and the Aleutian low weaken, while the Pacific high becomes more widespread. Strong westerly flow throughout the troposphere dominates most of the North Pacific basin, and northeasterly trade winds dominate the tropical latitudes. A comprehensive meteorological analysis of transport over the North Pacific during spring 2001 is presented by *Fuelberg et al.* [2003].

[31] The distribution of average (0–6 km) CO and ozone mixing ratios for the North American, Asian and European tagged tracers are shown in Figure 8, along with their respective horizontal fluxes. The concentrations and fluxes are averaged over the two and a half month time period of the 2001 PHOBEA-II campaign. Figure 9 shows the vertical distribution of concentrations and westerly fluxes of these tracers for a latitudinal cross-section at 125°W, along the west coast of North America.

5.1. North American Influence

[32] Over the Eastern United States, frontal lifting of North American boundary layer air towards the Atlantic is the dominant export pathway of pollution [*Prados et al.*, 1999; *Stohl and Trickl*, 1999; *Stohl*, 2001; *Cooper et al.*, 2002; *Li et al.*, 2002a]. A small fraction of North American pollution can also be exported to the Pacific through three
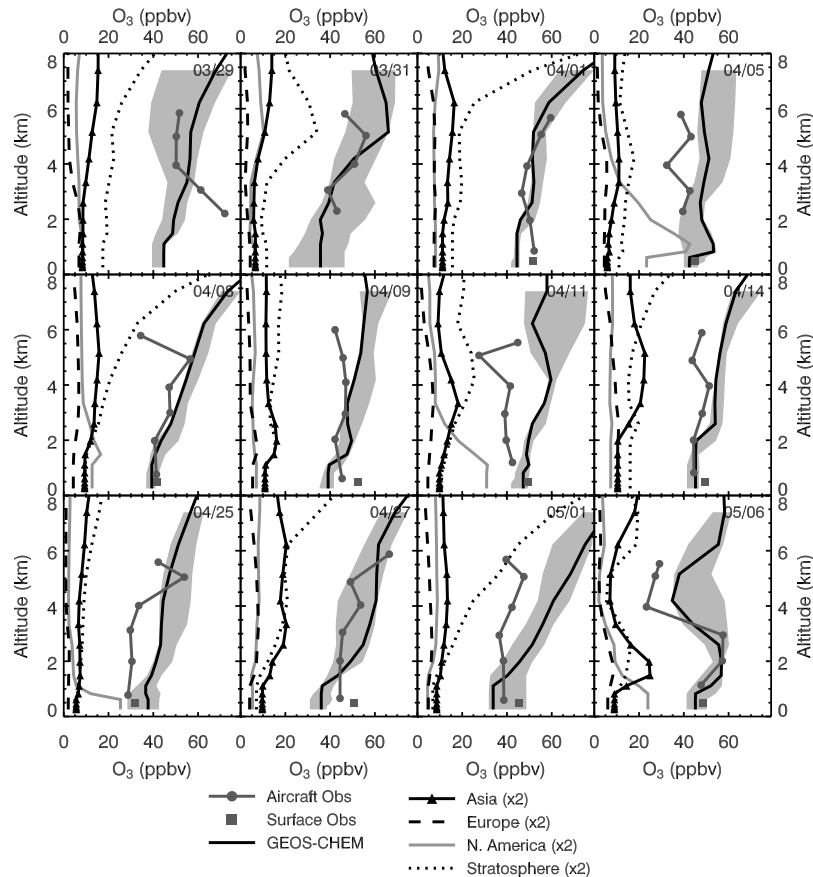
Figure 7. Ozone profiles during the 12 flights of the Duchess aircraft between 29 March and 6 May 2001. The observations (dark gray circles connected by gray lines) are compared with results from the GEOS-CHEM model (black lines) sampled at the time and location of the observations. The gray square symbols indicate simultaneous observations of CO at the ground. As in Figure 3, the light gray shading indicates the envelope of modeled profiles for nearby grid boxes within 6 hours of flight time. Individual contributions from Asian, North American, European, and stratospheric source regions from the tagged-O_x simulation are also shown. Note that the individual contributions have been scaled by a factor of two for clarity.

pathways: (1) episodic easterly low-level flow north of 40°N (discussed in section 4); (2) northeasterly flow on the southern branch of the Pacific high south of 30°N; and, (3) circumpolar circulation reaching the Pacific. These pathways result in 10–20 ppbv CO over the NE Pacific (Figure 8a). Westerly circumpolar transport through pathway (3) extends throughout the free troposphere, resulting in $1-2 \times 10^{-10}$ moles CO s^{-1} cm^{-2} between 2 and 10 km, while easterly transport via 1 and 2 occurs in the lower troposphere south of 30°N and north of 40°N (Figure 9a).

[33] The largest rates of springtime ozone production in North America occurs in the Eastern United States, colocated with large anthropogenic emissions of NO_x and NMHCs, resulting in North American O_3 levels greater than 30 ppbv. With its shorter lifetime due to photochemistry and surface deposition, North American O_3 is exported less efficiently relative to CO, contributing only 2–4 ppbv of ozone over the northern Pacific (Figure 8d). The largest influence is found off Baja California with up to 20 ppbv coming from anthropogenic American emissions (via pathway 2). The vertical distribution of North American ozone fluxes at 125°W (Figure 9d) shows that westerly transport

of North American ozone results in a $0.5-1 \times 10^{-10}$ moles O_3 s^{-1} cm^{-2} flux between 2 and 12 km (pathway 3), while stronger easterly fluxes (up to 2.5×10^{-10} moles O_3 s^{-1} cm^{-2}) occurs in the lower troposphere for latitudes south of 30°N (pathway 2), fueled by large rates of ozone production. Some of the ozone and CO transported through pathway 2 is entrained in the trade winds, and can thus influence the composition of the Northern Tropics [*Staudt et al.*, 2001].

5.2. Asian Influence

[34] *Liu et al.* [2003] and *Carmichael et al.* [2003] show that the major processes driving export of Asian anthropogenic pollution to the Pacific during spring 2001 are frontal lifting in warm conveyor belts (WCBs) ahead of cold fronts and boundary layer transport behind the cold fronts. The WCB is an ascending airstream ahead of a surface cold front [e.g., *Carlson*, 1980; *Browning*, 1999]. In addition, convection over South East Asia is important for driving the export of biomass burning emissions south of 30°N. Once over the Pacific, rapid westerly winds throughout the troposphere can transport Asian anthropogenic and biomass burning
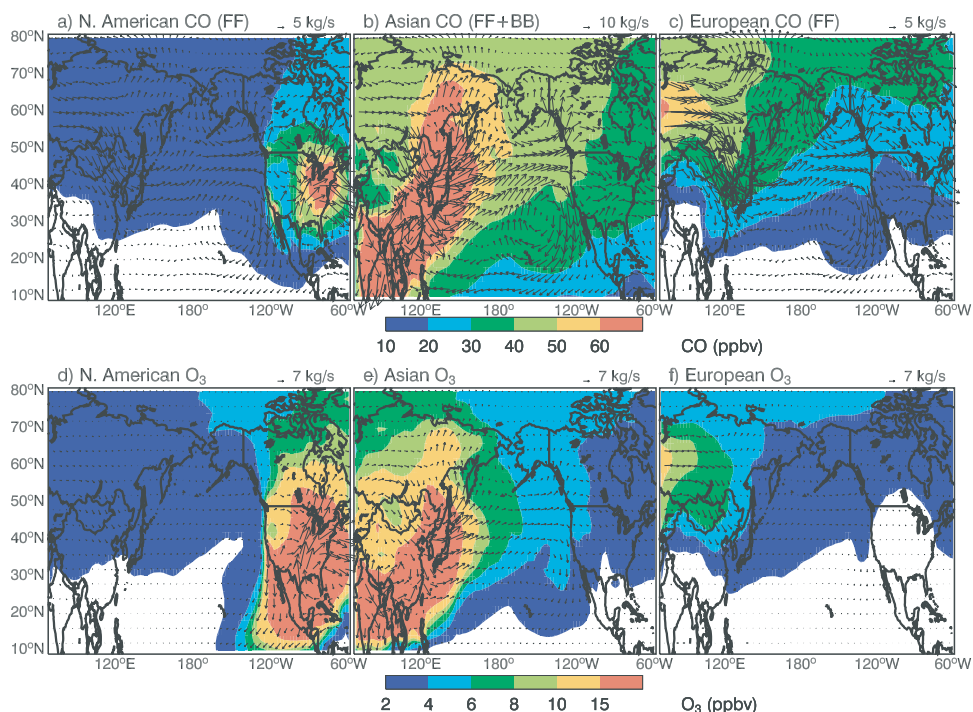
Figure 8. Modeled mean concentrations (0−6 km altitude) of North American, Asian, and European anthropogenic CO and ozone for 9 March−31 May 2001. The arrows represent the tracer horizontal mass fluxes between 0 and 6 km altitude.

effluents across the Pacific [*Jaffe et al.*, 1999; *Yienger et al.*, 2000].

[35] Asian sources account for 40−50 ppbv of CO in the NE Pacific troposphere (Figure 8b), roughly one third of the

total CO (Table 1), consistent with previous analyses [*Berntsen et al.*, 1999; *Yienger et al.*, 2000; *Staudt et al.*, 2001]. Most of this Asian CO originates from fossil fuel combustion, with only 5−10 ppbv coming from biomass
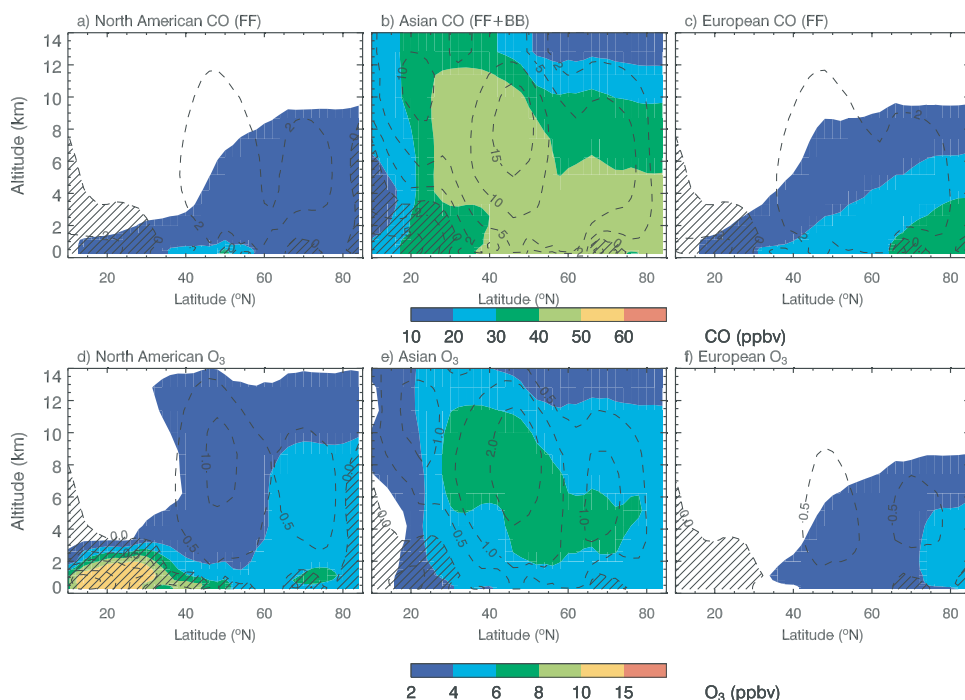
Figure 9. 9 March−31 May 2001 vertical cross section at 125°W of tagged CO and ozone fluxes (colored contours in ppbv) from North American, Asian and European anthropogenic sources. The dashed contour lines (in units of 10^{-10} moles s^{-1} cm^{-2}) represent horizontal fluxes of the tracers. Positive values are for westerly fluxes, while negative fluxes (hatched areas) represent easterly fluxes.

burning emissions, based on our climatological biomass burning emission inventory. Asian sources affect a large region of the NE Pacific, from the surface to 12 km altitude between 30 and 60°N (Figure 9b). This Asian influence shows a maximum at 4–10 km where warm conveyor belts deposit most of the transported CO [*Yienger et al.*, 2000; *Stohl*, 2001; *Liu et al.*, 2003]. At these altitudes the westerly fluxes reaches $10-15 \times 10^{-10}$ moles CO s^{-1} cm^{-2} (Figure 9b), but substantial fluxes ($>5 \times 10^{-10}$ moles CO s^{-1} cm^{-2}) are also reaching lower altitudes, illustrating the importance of boundary layer transport of Asian CO across the Pacific.

[36] Direct transport of surface ozone produced over Asia results in 4–6 ppbv of ozone in the NE Pacific, roughly 10% of total ozone (Figure 8e). Figure 9e shows a maximum Asian ozone contribution of 6–8 ppbv between 2 and 10 km altitude, induced by faster westerly transport at these altitudes and a longer lifetime for ozone.

[37] The Asian tagged O₃ tracer represents transport of ozone produced within the Asian lower troposphere but does not account for secondary ozone production via export of NO$_x$ and PAN from Asia. The difference between our standard full chemistry simulation and a simulation without Asian anthropogenic sources simulation (delta O₃, Figure 10) is a lower estimate of the combined direct transport and secondary ozone production from Asia (see section 2.3). By comparing Figures 10a and 8e, we find that the influence of secondary ozone production increases ozone by 2–4 ppbv on average in the NE Pacific for the 0–6 km column and is particularly significant in the areas influenced by the subsidence in the Pacific High pressure system as well as over the deserts in the Western U.S. where strong dry convection can entrain Asian pollution from aloft [*Jacob et al.*, 1999]. At the surface, there is only a 10–20% increase in ozone, reflecting the minor role of secondary production at low altitudes (compare Figure 10b with Figure 9e). In the upper troposphere over the eastern Pacific, secondary production results in a doubling of the Asian impact on ozone between 10 and 30°N. At these low latitudes, convection is the dominant export pathway from Asia [*Liu et al.*, 2003], and thus rapid lifting of Asian NO$_x$ followed by efficient ozone production during transport becomes a significant source of ozone.

5.3. European Influence

[38] Export of European pollution is generally confined to the lower troposphere below 3 km altitude [*Staudt et al.*, 2001], as a result of the high latitudes of emissions and the relative infrequency of cyclogenesis to efficiently vent the boundary layer [*Stohl*, 2001]. The main pathway for export of European pollution is northward to the Arctic [e.g., *Raatz*, 1989]. However, under the influence of the Siberian anticyclone, a fraction of European emissions is transported towards Asia [*Newell and Evans*, 2000; *Bey et al.*, 2001b], where it accounts for 30–50 ppbv CO and 4–6 ppbv of ozone (Figures 8c and 8f). After reaching the East coast of Asia, the pollution can then be exported to the Pacific in postfrontal boundary layer outflow where it mixes with Asian pollution [*Liu et al.*, 2003] and is carried in the storm track across the Pacific, mostly remaining at low altitudes and high latitudes (Figures 9c and 9f). This type of low-level transport is not efficient for ozone, which has a short
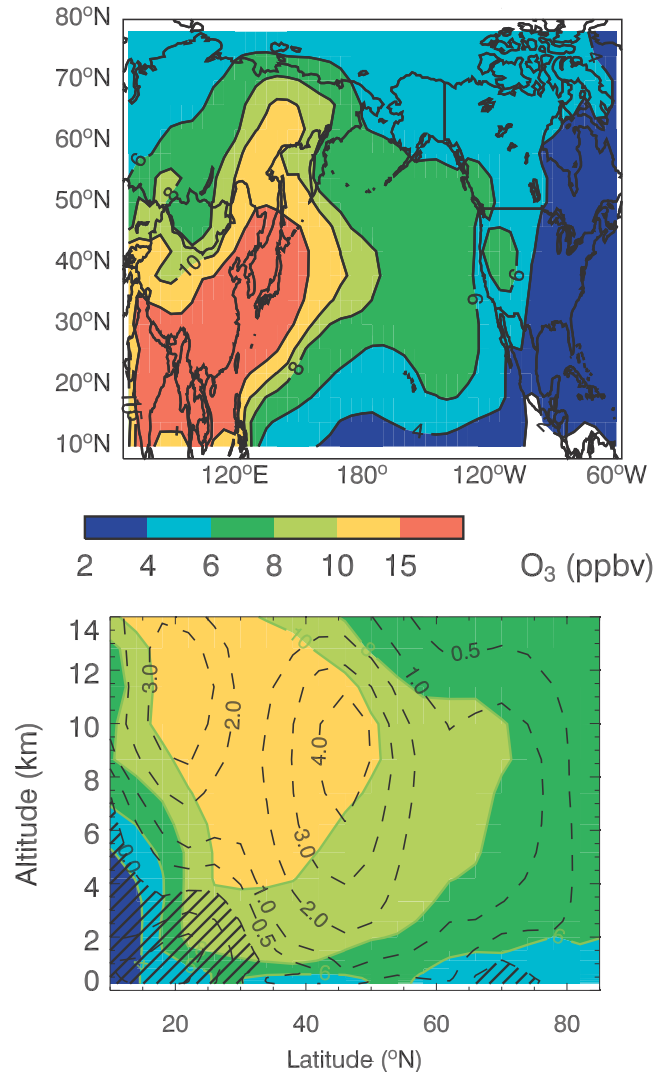

Figure 10. 9 March–31 May 2001 mean concentrations (0–6 km altitude) and vertical cross section at 125°W of Delta O₃ (= standard simulation-simulation without Asian emissions). Delta O₃ is a lower estimate of the combined direct transport and secondary ozone production from Asia.

lifetime in the lower troposphere; however, European CO can reach the United States. Overall the European influence results in 20–30 ppbv CO and 2–4 ppbv ozone in the NE Pacific (Figures 8c and 8f).

6. Origin of CO and Ozone at CPO

[39] Springtime CO concentrations at the CPO ground site are dominated by anthropogenic sources from Asia (43 ppbv), with significant contributions from North American (25 ppbv) and European (25 ppbv) sources (Figure 2, Table 1). The Asian contribution is mostly from fossil fuel and biofuel sources and only a small amount comes from biomass burning (7 ppbv). Most of the remaining CO comes from oxidation of methane and biogenic NMHCs. At the surface, 77% of the variability in the modeled CO is controlled by the variability in the North American source. Variability in Asian and European source contributions explain an additional 20% of the variability. Enhancements in

Table 2. Chemical Contributions to Odd-Oxygen (O$_x$) Over the Northeastern Pacific From the Tagged O$_x$ Simulation

Source Regions[a]	Northeastern Pacific: 0–6 km Column 35–60°N, 165°W–125°W	Cheeka Peak Observatory: 0–6 km Column 48.3°N, 124.8°W	Cheeka Peak Observatory: Mixing Ratios 48.3°N, 124.8°W, 480 m
Lower troposphere			
North America	3.6[b] (6%)	4.6[b] (8%)	6.5[c] (16%)
Europe	3.1 (5%)	2.9 (4.8%)	2.2 (5.5%)
Asia	7.6 (13%)	7.1 (12%)	4.4 (11%)
Pacific	8.7 (15%)	8.4 (14%)	9.5 (24%)
Others	4.5 (6%)	3.5 (5.2%)	2.6 (6.5%)
Middle troposphere	16.0 (27%)	17.0 (28%)	6.7 (17%)
Upper troposphere	7.2 (12%)	7.1 (12%)	3.2 (8%)
Stratosphere	9.3 (16%)	9.4 (16%)	4.9 (12%)
Total	60 (100%)	60 (100%)	40 (100%)

[a]Source regions are defined as: lower troposphere (700 hPa-surface), middle troposphere (700–400 hPa) and upper troposphere (400 hPa-tropopause). Subdivisions within the lower troposphere follow the same continental geographic regions defined in Table 1.
[b]Values are mean tropospheric columns (in 10^{16} molecules/cm^2) below 6 km altitude for 9 March–31 May 2001 from the tagged-O$_x$ simulation. Percentages are indicated in parenthesis.
[c]In this last column, values are in mixing ratios (in ppbv) for the tagged-O$_x$ simulation sampled at the location of CPO for 9 March–31 May 2001 (Figure 6).

Asian and European contributions often coincide (Figure 2), reflecting their mixing in post-frontal boundary layer outflow over the East Asian coast. With increasing altitude, the relative contributions from European and North American sources decrease while the Asian contribution increases (Figure 3).

[40] In contrast to CO, the Asian and European contributions to ozone levels are much smaller (Figures 6 and 7). At CPO, based on our tagged-ozone simulation, we find that 4 ppbv (11%) originate from production in the Asian lower troposphere (with an additional 1.5 ppbv coming from secondary production), while 2 ppbv (5%) come from Europe, and 6 ppbv (16%) from North America, as summarized in Table 2. The remaining contributions are mostly from chemical production over the Pacific, middle and upper troposphere, and stratosphere. The North American contribution explains 27% of the modeled ozone variability, while the Asian and European contributions together explain another 25% of ozone variability (the remaining variability is driven by stratospheric and free tropospheric sources). The model appears to overestimate the North American influence on ozone at CPO: increases in total ozone associated with the many high North American O$_3$ events in Figure 6 (coinciding with CO enhancements in Figure 2), are not present in the observations. Measurements at CPO during spring 1997 and 1998 [*Jaffe et al.*, 1999] often showed high concentrations of NO$_x$, PAN, and CO associated with observed ozone titration or lack of O$_3$ enhancement, during easterly flow from the nearby Seattle/Vancouver/Portland urban areas. With its 2° × 2.5° horizontal resolution, the model dilutes NO$_x$ emissions from nearby regions resulting in ozone production in the model. This overestimate of North American ozone production partly explains the poor correlation coefficient between model and observations (section 4). Given the model bias and poor correlation in reproducing the observed ozone we emphasize that our estimate of Eurasian source contributions for ozone is uncertain, but that we have much greater confidence in our estimate of Eurasian contributions to CO.

[41] How representative of the larger NE Pacific region are measurements made at the ground and above CPO? To answer this question we compare modeled tropospheric columns (up to 6 km) averaged over the NE Pacific (defined as 165–125°W; 35–65°N) to the columns at CPO (Tables 1 and 2). The CO columns are almost identical (CO: 15.8 × 10^{17} molecules/cm^2 in the NE Pacific, and 15.7 × 10^{17} molecules/cm^2 above CPO), implying that the 0–6 km column near CPO is indeed representative of the NE Pacific. The only difference comes from a slightly larger influence of North American contribution at the surface. The 0–6 km modeled O$_3$ columns above CPO are identical to the average O$_3$ columns over the NE Pacific (6 × 10^{17} molecules/cm^2), and in the tagged-ozone simulation, the North American influence dominates even more at CPO relative to the average NE Pacific columns (Table 2), but is likely to be due to the model's overestimate of North American influence noted above.

[42] Table 3 presents the terms contributing to the modeled O$_x$ budget in the NE Pacific during PHOBEA-II. We have subdivided the budget into three altitude regions: below 3 km altitude there is a net loss of O$_x$, between 3 and

Table 3. O$_x$ Budget Over the Northeastern Pacific[a]

	Budget		
	0–3 km	3–6 km	6–12 km
Chemistry			
Production	1.9	1.6	1.1
Loss	−2.2	−2.2	−0.8
Advection			
West	5.8	21	46.9
East	−4.8	−17.4	−39.2
North	−1.3	−2.7	−3.6
South	−1.3	−1.2	−4.4
Vertical transport			
Top	1.9	2.5	3.2
Bottom	0.0	−1.9	−2.6
Deposition			
Wet	−0.5	−0.1	−0.02
Dry	−0.7	0.0	0.0
Net	−1.2	−0.4	0.6

[a]Results are from the full chemistry simulation. Values are in Gmoles/day for 9 March–31 May 2001 averaged over the NE Pacific (35–60°N, 165°W–125°W). Positive values correspond to net sources for that region.
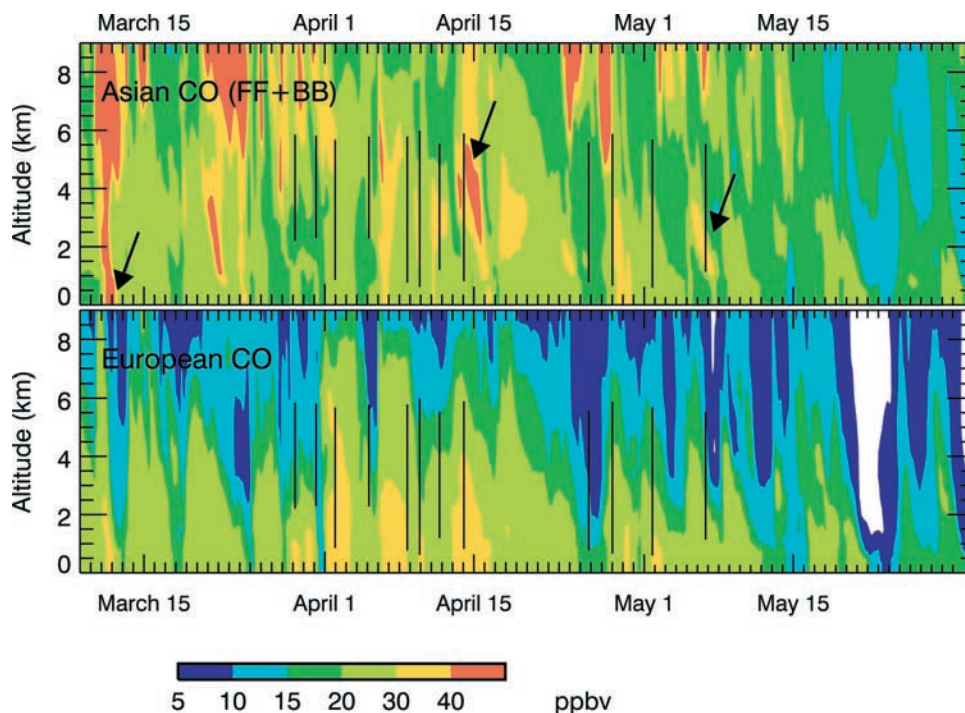
Figure 11. Time height cross section of Asian and European contributions to CO (in ppbv) at CPO. The vertical lines show the timing and vertical extent of PHOBEA-II flights. The arrows indicate the three long-range transport events discussed in section 7 (11 March, 14 April, and 6 May 2001).

6 km altitude the O_x budget is nearly balanced, and between 6 and 12 km altitude there is a net production of O_x. In the lower part of the troposphere (<3 km), the O_x sources are controlled by advection from the west, descent from higher altitudes, and photochemical production. These sources are more than balanced by sinks in the form of advection out of the region through the East, North and South, deposition, and photochemical loss. Subsidence in the Pacific High pressure system appears as an important mechanism for supplying O_x to the NE Pacific lower troposphere. In the middle and upper troposphere the dominant O_x source is westerly advection, which increases with increasing altitude. Below 6 km there is net photochemical loss of ozone in NE Pacific region, consistent with the photochemical box model analysis of *Kotchenruther et al.* [2001b].

7. Case Studies of Trans-Pacific Transport of Pollutants

[43] The episodic nature of trans-Pacific transport [e.g., *Jaffe et al.*, 1999; *Yienger et al.*, 2000; *Hess et al.*, 2000] can be clearly seen at CPO in Figures 2 and 5, as well as in Figure 11, which shows the time-height dependence of Asian and European contributions to CO above CPO. Strong long-range transport episodes with Asian CO > 60 ppbv occur on 12 separate times (see Figure 11) and are seen much more frequently in the middle and upper troposphere compared with the lower troposphere, where only one such episode is predicted by the model, on 11 March 2001. This lower tropospheric long-range transport episode resulted in an increase in CO observed at CPO, lending confidence to the model transport (arrow on Figure 2). Two other Asian long-range transport episodes

with smaller CO enhancements can also be noted in the surface observations and the model on Figures 2 and 11: 6–8 April and 28–29 April 2001. *Jaffe et al.* [2003] identified three episodes of long-range transport in the spring 2001 PHOBEA-II aircraft profiles for 29 March, 14 April, and 6 May. Significant gas and aerosol layers were observed on all three flights. Back trajectories suggest an Asian source region while the gas and aerosol composition suggest industrial sources sometimes accompanied by mineral dust sources. The GEOS-CHEM model misses the 29 March event. However, the model does capture the 14 April and 6 May cases (Figures 3 and 7), and attributes the CO enhancements to transport of Asian pollution, consistent with the interpretation of *Jaffe et al.* [2003]. We now focus on a case-by-case analysis of these three long-range transport events which were observed in the NE Pacific and captured by the model: 11 March, 14 April, and 6 May 2001.

7.1. 11 March 2001

[44] The 11 March 2001 event is unique in two respects: the large contribution from Asian sources, exceeding 60 ppbv of CO at the ground (Figure 2), and the vertical extent of the enhancement, which occurred throughout the troposphere, reaching a maximum of 115 ppbv Asian CO at 6 km altitude (Figure 11). Figure 5 shows a 30% increase in modeled column CO below 6 km altitude. NOAA HYSPLIT [*Draxler and Hess*, 1997] back trajectory calculations (not shown) indicate low-level transport from Asia with a transit time of 7 days at the surface, and a more rapid transit in the middle troposphere, confirming the GEOS-CHEM results. The observations exhibited enhanced CO for a 24-hour time period (~30 ppbv enhancement relative to mean spring levels) but no enhancements in
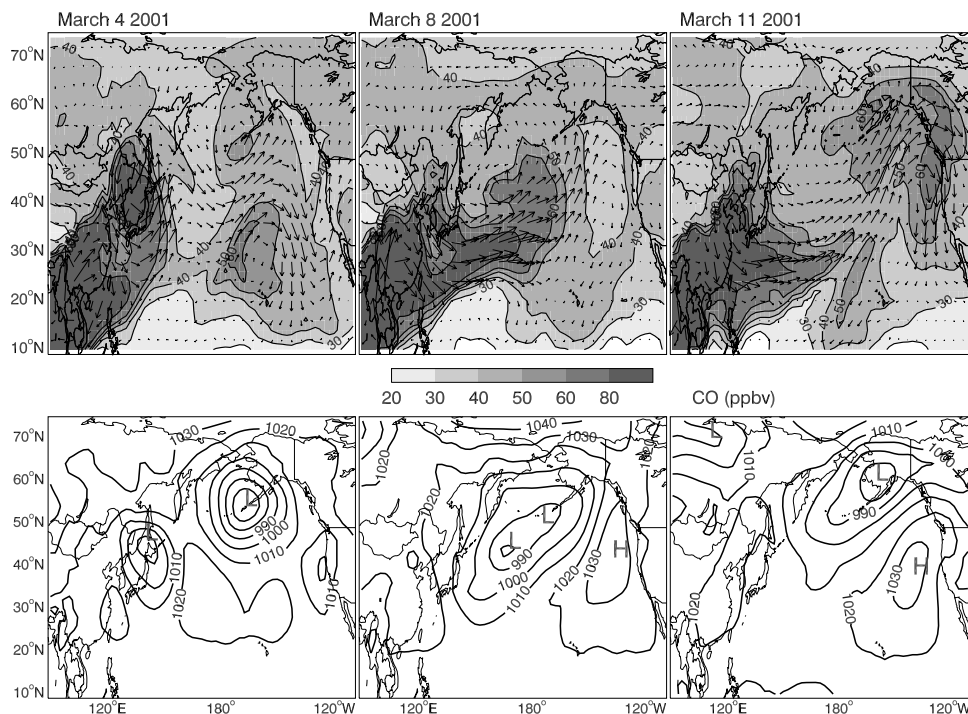
Figure 12. (top) Daily Asian CO mixing ratios (in ppbv, colored contours) averaged between 0 and 6 km for 4 March, 8 March, and 11 March 2001. The arrows show averaged horizontal fluxes. (bottom) Sea level pressure for 4 March, 8 March, and 11 March 2001.

ozone or aerosols. The model captures the timing of this event remarkably well but somewhat underestimates the increase in CO (Figure 2). The model also predicts an increase in Asian ozone to 8 ppbv (Figure 6). These are the largest levels of Asian ozone calculated at CPO for spring 2001, but the resulting small increase (~5 ppbv) in ozone on top of the background levels is difficult to identify in the total modeled ozone levels, consistent with lack of enhancement in the O₃ observations.

[45] This long-range transport event has its origin in an intrusion of cold mid-latitude air deep into the South China Sea in early March 2001. This "cold-surge" was associated with a surface cold front extending to northern Japan. Using the GEOS-CHEM model, *Liu et al.* [2003] find that outflow of Asian pollution over South China occurred both in the warm conveyor belt ahead of this cold front, as well as in the boundary layer behind the front. This cold surge lead to the highest eastward flux of CO in the lower free troposphere over the western Pacific in spring 2001.

[46] Figure 12, presenting average mixing ratios of Asian CO between 0 and 6 km as well as horizontal fluxes and sea level pressure maps, illustrates the sequence of events between 4 March and 11 March 2001. The low pressure system at 42°N, 150°E forced Asian pollution outflow over the Pacific to the northeast, with maximum horizontal fluxes between 25° and 40°N on 4 March. Over the next few days the cyclone traveled on a northeast trajectory in the Pacific storm track and merged with another cyclone forming over the Gulf of Alaska. By 8 March, the Asian CO was located in the lower troposphere behind the cold front, as well as ahead of the cold front in the warm conveyor belt, where it ascended to the middle troposphere with a southerly flow.

On 7 and 9 March, the TRACE-P DC-8 aircraft flew out of Hong Kong across the cold front. Lifting of Asian CO ahead of the cold front between 4 and 8 km altitude was apparent in both observations and in model simulations [*Liu et al.*, 2003; *Carmichael et al.*, 2003]. Strong subsidence capped the high levels of CO observed in the boundary-layer outflow behind the cold front.

[47] Strong wind speeds throughout the troposphere allowed rapid transport of this Asian pollution across the Pacific. The upper tropospheric leading edge of the Asian CO tracer, traveling in the warm conveyor belt, reached the North American coast on 10 March at 12 GMT (Figure 11). It was followed one day later by the lower tropospheric Asian CO, channeled between the low pressure system over the Gulf of Alaska and the Pacific high (Figure 12). By that time some of the upper tropospheric Asian CO started subsiding on the east side of the Pacific anticyclone off the Oregon and California coasts.

7.2. 14 April 2001

[48] The 14 April case was discussed by *Price et al.* [2003] and *Jaffe et al.* [2003] and appears to have started as a large dust storm induced by a low-pressure system passing over the Gobi desert on 6 April 2001 [*Gong et al.*, 2003]. Over the next few days the system intensified and moved towards northeast Asia, passing over areas with high anthropogenic emissions. It then rapidly crossed the Pacific, and on 13 April the leading edge of the pollution plume reached the Washington and Oregon coasts between 2 and 6 km altitude (Figures 1 and 11).

[49] On 14 April the observed CO was significantly enhanced between 4 and 6 km altitude, reaching 173 ppbv, but ozone showed little to no enhancement (Figure 7). The
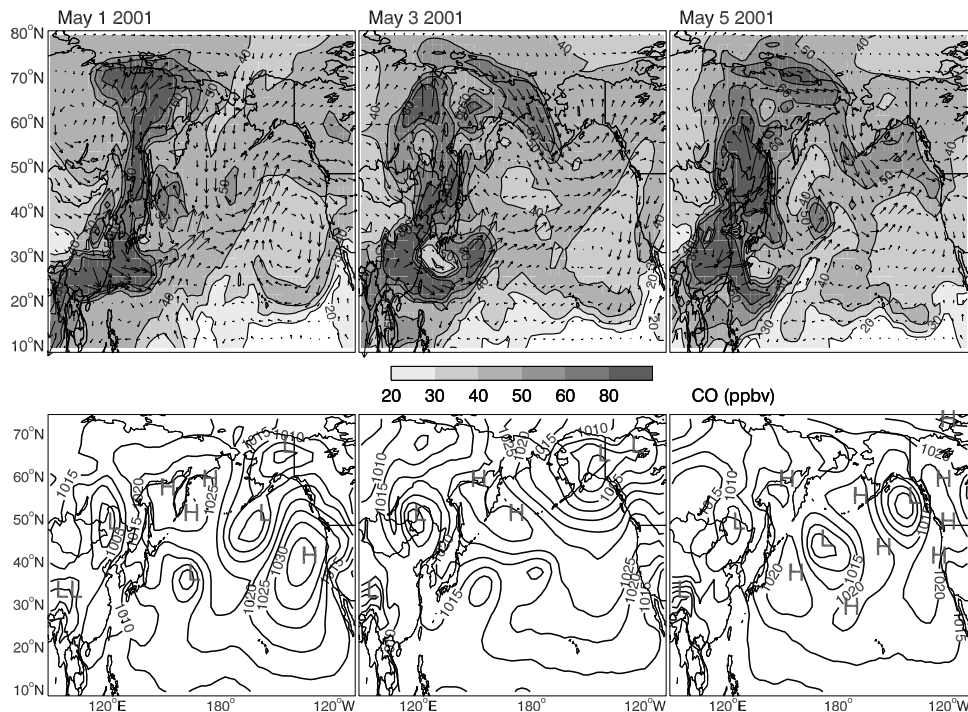
Figure 13. (top) Daily Asian CO mixing ratios (in ppbv, colored contours) at 2.5 km (740 hPa) for 1, 3, and 5 May 2001. The arrows show averaged horizontal fluxes. (bottom) Sea level pressure for 1, 3, and 5 May 2001.

GEOS-CHEM model predicts a somewhat smaller CO enhancement displaced to lower altitudes (3–5 km) resulting from Asian CO. The model also somewhat underestimates the lower tropospheric maximum and attributes it to a combination of Asian and European influences (Figures 2 and 3). In fact European influence on CO was the highest calculated at CPO for spring 2001 (40 ppbv), however the simultaneous decrease in Asian contribution resulted in no overall increase in total modeled CO levels, consistent with observations. This European CO plume traveled below the Asian plume and was initially exported over the Pacific behind the low pressure system ahead of the one which caused the dust storm. By 13 April the Asian plume, which is traveling at higher altitudes, has caught up with the European plume and both are arriving over North America at the same time.

7.3. 6 May 2001

[50] During the last days of April, the Siberian anticyclone extended to the East, over the Sea of Okhotsk, where it remained stationary for the first few days of May (Figure 13). As a cyclone approached this blocking high from the west on 1 May, the strong pressure gradients between the two systems forced a northward surge of Asian pollution towards the Arctic. The Asian pollution traveled at low levels on the western and northern sides of the anticyclone. It then came under the influence of a developing surface low pressure system over Alaska and was rapidly transported along a northwesterly trajectory to the NE Pacific. Because the Asian anticyclone was the dominant pressure system guiding the export of Asian pollution, most of the transport initially remained at low levels. This is consistent with the

backtrajectory analysis of *Price et al.* [2003] for this 6 May event, indicating a high-latitude Eurasian origin for air below 3 km altitude and an aged marine origin above.

[51] On 6 May the GEOS-CHEM model captures the observed CO and ozone enhancements between 1 and 3 km altitude (Figures 3 and 7). The CO enhancement is attributed to Asian sources. For ozone, the model assigns the increase to a combination of a strong Asian component and a stratospheric contribution. The northerly route (compared with the 11 March case) precluded strong photochemical loss of ozone, thus explaining the large 12–15 ppbv Asian ozone above CPO (Figure 7). The stratospheric intrusion was associated with the upper-level cut-off low and mixed in with the Asian pollution prior to its arrival over CPO. We confirmed the stratospheric origin of the air by examining TOMS total ozone satellite images, and by identifying dry air in GOES-West channel 2 water vapor imagery. The nearby Quillayute, Washington (47.95°N, 124.55°W) sounding indicated that the stratospheric intrusion occurred between 1.5 and 3 km altitude, consistent with the modeled ozone profiles in Figure 7.

8. Conclusions

[52] During the PHOBEA-II project, continuous observations of CO, ozone, and aerosols were obtained between 9 March and 31 May 2001 at the Cheeka Peak Observatory (48.3°N, 124.6°W, 480 m), a coastal site in Washington State. These observations were complemented by twelve vertical profiles (0–6 km) conducted above CPO with a twin-engine Beechcraft Duchess aircraft. The PHOBEA-II project took place at the same time as the TRACE-P and

ACE-Asia field missions, which both sampled the western north Pacific troposphere. The GEOS-CHEM chemical transport model forecasts were successfully used not only to probe a number of trans-Pacific pollution transport episodes in the NE Pacific but also to gather a representative dataset throughout the spring.

[53] The GEOS-CHEM model provides a very good simulation of CO observations both at the ground and aloft, reproducing average levels and day-to-day variability. The model's ability in capturing CO observations strongly suggests a good understanding of CO sources (in particular Asian sources), loss, and transport mechanisms, consistent with the analysis of *Palmer et al.* [2003] and Heald et al. (submitted manuscript, 2003).

[54] For ozone, the model underestimates the ground-based observations by 8 ppbv, overestimates the aircraft profiles by 5 ppbv, and does not capture the temporal variability of the observations. These model biases could be due the assumption of a uniform $\gamma_{N2O5} = 0.03$ for the heterogeneous reaction $N_2O_5 + H_2O \rightarrow 2HNO_3$ on aerosols (laboratory measurements indicate a strong temperature and relative humidity dependence for γ_{N2O5}) or could also be due to misrepresentation of stratosphere-troposphere exchange during spring 2001 and uncertainties in NO_x emission inventories. The poor correlation between observed and modeled ozone reflects the lack of variability in the observations and an apparent model overestimate of nearby North American influence on ozone because of the model's coarse horizontal resolution.

[55] With GEOS-CHEM simulations tagging CO and ozone according to source regions, we examined the impact of Asian and European sources on the composition of the NE Pacific troposphere. We find that 33% of CO in the 0–6 km near CPO comes from Asian sources and 15% from European sources, while North American sources account for 11%. The Asian contribution increases with increasing altitude, while the North American and European contributions decrease. At the surface, North American CO sources become more important (17%) and account for 77% of the variability in CPO observations. In the 0–6 km column near CPO, direct transport of ozone produced over Asia and Europe respectively account for 12% and 5% of ozone. We estimate that the full contribution from Asian emissions to O₃ in the 0–6 km column (including secondary production of ozone from export of Asian PAN and NO_x to the free troposphere) is at least 16%. Given the poor performance of the model in reproducing O₃ observations, a large uncertainty is associated with our calculation of O₃ source contributions. However, we have greater confidence in our estimate of Eurasian contributions to CO because of the very good agreement with observations.

[56] We find that the budget of odd-oxygen in the NE Pacific below 6 km is characterized by net loss: photochemical loss and deposition are partly counterbalanced by westerly advection and photochemical production. Above 6 km there is net photochemical production of ozone in NE Pacific region.

[57] Based on back trajectory calculations combined with observed layers of enhanced gases and aerosols, *Jaffe et al.* [2003] identified three episodes of long-range transport of air pollutants and dust from Asia in the PHOBEA-II aircraft observations. The GEOS-CHEM model captures two of these episodes and confirms the Asian origin of these airmasses. Using the tagged CO simulation, we identified an additional long-range transport event in the surface observations at CPO and linked it to strong post-frontal boundary layer outflow observed 4 days earlier in the western Pacific during TRACE-P [*Liu et al.*, 2003; *Carmichael et al.*, 2003]. In all three cases reproduced by the model, both observations and model show clear enhancements in CO. However, only in one of these cases is ozone enhanced. This enhancement is captured by the model and is attributed to a combination of transport of Asian ozone at high latitudes and ozone of stratospheric origin. In the other two cases, the modeled contribution from Asian ozone increases to 8–10 ppbv but the total levels of ozone are not significantly enhanced, rendering detection of Asian influence on ozone difficult.

References

Akimoto, H., and H. Narita, Distribution of SO_2, NO_x, and CO_2 emissions from fuel combustion and industrial activities in Asia with $1° \times 1°$ resolution, *Atmos. Environ.*, 28, 213–225, 1994.

Andreae, M. O., H. Berresheim, T. W. Andreae, M. A. Kritz, T. S. Bates, and J. T. Merrill, Vertical distribution of dimethylsulfide, sulfur dioxide, aerosol ions, and radon over the northeast Pacific Ocean, *J. Atmos. Chem.*, 6, 149–173, 1988.

Benkovitz, C. M., T. Scholtz, J. Pacyna, L. Tarrasn, J. Dignon, E. Voldner, P. A. Spiro, J. A. Logan, and T. E. Graedel, Global inventories of anthropogenic emissions of SO_2 and NO_x, *J. Geophys. Res.*, 101, 29,239–29,253, 1996.

Berntsen, T. K., S. Karlsdottir, and D. A. Jaffe, Influence of Asian emissions on the composition of air reaching the northwestern United States, *Geophys. Res. Lett.*, 26, 2171–2174, 1999.

Bey, I., D. J. Jacob, R. M. Yantosca, J. A. Logan, B. D. Field, A. M. Fiore, Q. Li, H. Y. Liu, L. J. Mickley, and M. G. Schultz, Global modeling of tropospheric chemistry with assimilated meteorology: Model description and evaluation, *J. Geophys. Res.*, 106, 23,073–23,096, 2001a.

Bey, I., D. J. Jacob, J. A. Logan, and R. M. Yantosca, Asian chemical outflow to the Pacific: Origins, pathways, and budgets, *J. Geophys. Res.*, 106, 23,097–23,114, 2001b.

Bognar, J. A., and J. W. Birks, Miniaturized ultraviolet ozonesonde for atmospheric measurements, *Anal. Chem.*, 68, 3059–3062, 1996.

Browning, K. A., Mesoscale aspects of extratropical cyclones: An observational perspective, in *The Life Cycles of Extratropical Cyclones*, edited by M. A. Shapiro and S. Gronas, Am. Meteorol. Soc., Boston, Mass., 1999.

Carlson, T. N., Airflow through midlatitude cyclones and the comma cloud pattern, *Mon. Weather Rev.*, 108, 1498–1509, 1980.

Carmichael, G. R., I. Uno, M. J. Phadnis, Y. Zhang, and Y. Sunwoo, Tropospheric ozone production and transport in the springtime in east Asia, *J. Geophys. Res.*, 103, 10,649–10,671, 1998.

Carmichael, G. R., et al., Regional-scale chemical transport modeling in support of intensive field experiments: Overview and analysis of the TRACE-P observations, *J. Geophys. Res.*, 108(D21), 8823, doi:10.1029/2002JD003117, in press, 2003.

Cooper, O. R., J. L. Moody, D. D. Parrish, M. Trainier, T. B. Ryerson, J. S. Holloway, G. Hubler, F. C. Fehsenfeld, and M. J. Evans, Trace gas composition of midlatitude cyclones over the western North Atlantic Ocean: A conceptual model, *J. Geophys. Res.*, 107(D7), 4056, doi:10.1029/2001JD000901, 2002.

Dentener, F. J., and P. J. Crutzen, Reaction of N_2O_5 on tropospheric aerosols: Impact on the global distributions of NO_x, O_3, and OH, *J. Geophys. Res.*, 98, 7149–7163, 1993.

Dickerson, R. R., S. Kondragunta, G. Stenchikov, K. L. Civerolo, B. G. Doddridge, and B. N. Holben, The impact of aerosols on solar ultraviolet radiation and photochemical smog, *Science*, 278, 827–830, 1997.

Draxler, R. R., and G. D. Hess, Description of the Hysplit_4 modeling system, *NOAA Tech. Memo ERL ARL-224*, Natl. Ocean. and Atmos. Admin., Silver Spring, Md., 1997.

Duncan, B. N., R. V. Martin, A. C. Staudt, R. M. Yevich, and J. A. Logan, Interannual and seasonal variability of biomass burning emissions constrained by remote-sensed observations, *J. Geophys. Res.*, *108*(D2), 4040, doi:10.1029/2002JD002378, 2003.

Elliott, S., D. R. Blake, R. A. Duce, C. A. Lai, I. McCreary, L. A. McNair, F. S. Rowland, A. G. Russell, G. E. Streit, and R. P. Turco, Motorization of China implies changes in Pacific air chemistry and primary production, *Geophys. Res. Lett.*, *24*, 2671–2674, 1997.

Fiore, A. M., D. J. Jacob, I. Bey, R. M. Yantosca, B. D. Field, A. C. Fusco, and J. G. Wilkinson, Background ozone over the United States in summer: Origin, trend and contributions to pollution episodes, *J. Geophys. Res.*, *107*(D15), 4275, doi:10.1029/2001JD000982, 2002.

Fuelberg, H. E., C. M. Kiley, J. R. Hannan, D. J. Westberg, M. A. Avery, and R. E. Newell, Atmospheric transport during the Transport and Chemical Evolution Experiment over the Pacific (TRACE-P) experiment, *J. Geophys. Res.*, *108*(D20), 8782, doi:10.1029/2002JD003092, in press, 2003.

George, C., J. L. Ponche, P. Mirabel, W. Behnke, V. Sheer, and C. Zetzsch, Study of the uptake of N₂O₅ by water and NaCl solutions, *J. Phys. Chem.*, *98*, 8780–8784, 1994.

Gong, S. L., X. Y. Zhang, T. L. Zhao, I. G. McKendry, D. A. Jaffe, and N. M. Lu, Characterization of soil dust aerosol in China and its transport/distribution during 2001 ACE-Asia: 2. Model simulation and validation, *J. Geophys. Res.*, *108*(D9), 4262, doi:10.1029/2002JD002633, 2003.

Hallquist, M., D. J. Stewart, J. Baker, and R. A. Cox, Hydrolysis of N₂O₅ on submicron sulfuric acid aerosols, *J. Phys. Chem. A*, *104*, 3984–3990, 2000.

He, S., and G. R. Carmichael, Sensitivity of photolysis rates and ozone production in the troposphere to aerosol properties, *J. Geophys. Res.*, *104*, 26,307–26,324, 1999.

Heald, C. L., D. J. Jacob, P. I. Palmer, M. J. Evans, G. W. Sachse, H. B. Singh, and D. R. Blake, Biomass burning emission inventory with daily resolution: Application to aircraft observations of Asian outflow, *J. Geophys. Res.*, *108*(D4), 8368, doi:10.1029/2002JD002732, 2003.

Hess, P. G., S. Flocke, J.-F. Lamarque, M. C. Barth, and S. Madronich, Episodic modeling of the chemical structure of the troposphere as revealed during the spring MLOPEX 2 intensive, *J. Geophys. Res.*, *105*, 26,809–26,840, 2000.

Hu, J. H., and J. P. D. Abbatt, Reaction probabilities for N₂O₅ hydrolysis on sulfuric acid and ammonium sulfate aerosols at room temperature, *J. Phys. Chem.*, *101*, 871–878, 1997.

Huebert, B., T. Bates, P. Russell, J. Seinfeld, M. Wang, M. Uematsu, and Y. J. Kim, An overview of ACE-Asia: Strategies for quantifying the relationships between Asian aerosols and their climatic impacts, *J. Geophys. Res.*, *108*, doi:10.1029/2003JD003550, in press, 2003.

Husar, R. B., et al., The Asian dust events of April 1998, *J. Geophys. Res.*, *106*, 18,317–18,333, 2001.

Jacob, D. J., Heterogeneous chemistry and tropospheric ozone, *Atmos. Environ.*, *34*, 2131–2159, 2000.

Jacob, D. J., J. A. Logan, and P. P. Murti, Effect of rising Asian emissions on surface ozone in the United States, *Geophys. Res. Lett.*, *26*, 2175–2178, 1999.

Jacob, D. J., J. H. Crawford, M. M. Kleb, V. S. Connors, R. J. Bendura, J. L. Raper, G. W. Sachse, J. C. Gille, L. Emmons, and C. L. Heald, The Transport and Chemical Evolution over the Pacific (TRACE-P) aircraft mission: Design, execution, and first results, *J. Geophys. Res.*, *108*(D20), 8781, doi:10.1029/2002JD003276, in press, 2003.

Jaffe, D. A., et al., Transport of Asian air pollution to North America, *Geophys. Res. Lett.*, *26*, 711–714, 1999.

Jaffe, D. A., T. Anderson, D. Covert, B. Trost, J. Danielson, W. Simpson, D. Blake, and J. Harris, Observations of ozone and related species in the northeast Pacific during the PHOBEA campaigns: 1. Ground-based observations at Cheeka Peak, *J. Geophys. Res.*, *106*, 7449–7461, 2001.

Jaffe, D. A., I. McKendry, T. Anderson, and H. Price, Six new episodes of trans-Pacific transport of air pollutants, *Atmos. Environ.*, *37*, 391–404, 2003.

Kane, S. M., F. Caloz, and M.-T. Leu, Heterogeneous uptake of gaseous N₂O₅ by (NH₄)₂SO₄, NH₄HSO₄, and H₂SO₄ aerosols, *J. Phys. Chem.*, *105*, 6465–6470, 2001.

Kiley, C. M., et al., An intercomparison and validation of aircraft-derived and simulated CO from seven chemical transport models during the TRACE-P experiment, *J. Geophys. Res.*, *108*(D21), 8819, doi:10.1029/2002JD003089, in press, 2003.

Kotchenruther, R. A., D. A. Jaffe, H. J. Beine, T. L. Anderson, J. W. Bottenheim, J. M. Harris, D. R. Blake, and R. Schmitt, Observations of ozone and related species in the northeast Pacific during the PHOBEA campaigns: 2. Airborne observations, *J. Geophys. Res.*, *106*, 7463–7483, 2001a.

Kotchenruther, R., D. A. Jaffe, and L. Jaeglé, Ozone photochemistry and the role of PAN in the springtime northeastern Pacific troposphere: Results from the PHOBEA campaign, *J. Geophys. Res.*, *106*, 28,731–28,743, 2001b.

Kritz, M. A., J. C. LeRoulley, and E. F. Danielsen, The China Clipper: Fast advective transport of radon-rich air form the Asian boundary layer to the upper troposphere near California, *Tellus*, *42B*, 46–61, 1990.

Lee, S.-H., H. Akimoto, H. Nakane, S. Kurnosenko, and Y. Kinjo, Lower tropospheric ozone trend observed in 1989–1997 at Okinawa, Japan, *Geophys. Res. Lett.*, *25*, 1637–1640, 1998.

Li, Q., et al., Transatlantic transport of pollution and its effects on surface ozone in Europe and North America, *J. Geophys. Res.*, *107*(D13), 4166, doi:10.1029/2001JD001422, 2002a.

Li, Q., D. J. Jacob, T. D. Fairlie, H. Liu, R. M. Yantosca, and R. V. Martin, Stratospheric versus pollution influences on ozone at Bermuda: Reconciling past analyses, *J. Geophys. Res.*, *107*(D22), 4611, doi:10.1029/2002JD002138, 2002b.

Liao, H., Y. L. Yung, and J. H. Seinfeld, Effects of aerosols on tropospheric photolysis rates in clear and cloudy atmospheres, *J. Geophys. Res.*, *104*, 23,697–23,707, 1999.

Liu, H., D. J. Jacob, L. Y. Chan, S. J. Oltmans, I. Bey, R. M. Yantosca, J. M. Harris, B. N. Duncan, and R. V. Martin, Sources of tropospheric ozone along the Asian Pacific Rim: An analysis of ozonesonde observations, *J. Geophys. Res.*, *107*(D21), 4573, doi:10.1029/2001JD002005, 2002.

Liu, H., D. J. Jacob, I. Bey, R. M. Yantosca, B. N. Duncan, and G. W. Sachse, Transport pathways for Asian combustion outflow over the Pacific: Interannual and seasonal variations, *J. Geophys. Res.*, *108*(D20), 8786, doi:10.1029/2002JD003102, in press, 2003.

Logan, J. A., Trends in the vertical distribution of ozone: An analysis of ozone sonde data, *J. Geophys. Res.*, *99*, 25,553–25,585, 1994.

Logan, J. A., M. J. Prather, S. C. Wofsy, and M. B. McElroy, Tropospheric chemistry: A global perspective, *J. Geophys. Res.*, *86*, 7210–7254, 1981.

Martin, R. V., et al., Interpretation of TOMS observations of tropical tropospheric ozone with a global model and in-situ observations, *J. Geophys. Res.*, *107*(D18), 4351, doi:10.1029/2001JD001480, 2002.

Martin, R. V., D. J. Jacob, R. M. Yantosca, M. Chin, and P. Ginoux, Global and regional decreases in tropospheric oxidants from photochemical effects of aerosols, *J. Geophys. Res.*, *108*(D3), 4097, doi:10.1029/2002JD002622, 2003.

McKendry, I. G., J. P. Hacker, and R. Stull, Long-range transport of Asian dust to the Lower Fraser Valley, British Columbia, Canada, *J. Geophys. Res.*, *106*, 18,361–18,370, 2001.

McLinden, C. A., S. Olsen, B. Hannegan, O. Wild, M. J. Prather, and J. Sundet, Stratospheric ozone in 3-D models: A simple chemistry and the cross-tropopause flux, *J. Geophys. Res.*, *105*, 14,653–14,665, 2000.

Mentel, T. F., M. Sohn, and A. Wahner, Nitrate effect in the heterogeneous hydrolysis of dinitrogen pentoxide on aqueous aerosols, *Phys. Chem. Chem. Phys.*, *24*, 5451–5457, 1999.

Mozurkewich, M., and J. G. Calvert, Reaction probability of N₂O₅ on aqueous aerosols, *J. Geophys. Res.*, *93*, 15,889–15,896, 1988.

Newell, R. E., and M. J. Evans, Seasonal changes in pollutant transport to the North Pacific: The relative importance of Asian and European sources, *Geophys. Res. Lett.*, *27*, 2509–2512, 2000.

Palmer, P. I., D. J. Jacob, K. Chance, R. V. Martin, R. J. D. Spurr, T. P. Kurosu, I. Bey, R. Yantosca, A. Fiore, and Q. Li, Air mass factor formulation for spectroscopic measurements from satellites: Application to formaldehyde retrievals from GOME, *J. Geophys. Res.*, *106*, 14,539–14,550, 2001.

Palmer, P. I., D. J. Jacob, D. B. A. Jones, C. L. Heald, R. M. Yantosca, J. A. Logan, G. W. Sachse, and D. G. Streets, Inverting for emissions of carbon monoxide from Asia using aircraft observations over the western Pacific, *J. Geophys. Res.*, *108*(D21), 8828, doi:10.1029/2002JD003397, in press, 2003.

Parrish, D. D., C. J. Hahn, E. J. Williams, R. B. Norton, F. C. Fehsenfeld, H. B. Singh, J. D. Shetter, B. W. Gandrud, and B. A. Ridley, Indications of photochemical histories of Pacific air masses from measurements of atmospheric trace species at Pt. Arena, California, *J. Geophys. Res.*, *97*, 15,883–15,901, 1992.

Piccot, S. D., J. J. Watson, and J. W. Jones, A global inventory of volatile organic compound emissions from anthropogenic sources, *J. Geophys. Res.*, *97*, 9897–9912, 1992.

Prados, A. I., R. R. Dickerson, B. G. Doddridge, P. A. Milne, J. L. Moody, and J. T. Merrill, Transport of ozone and pollutants from North America to the North Atlantic Ocean during the 1996 Atmosphere/Ocean Chemistry Experiment (AEROCE) intensive, *J. Geophys. Res.*, *104*, 26,219–26,233, 1999.

Prather, M. J., and D. Ehhalt, Atmospheric chemistry and greenhouse gases, in *Climate Change 2001: The Science of Climate Change*, Cambridge Univ. Press, New York, 2001.

Price, H. U., D. A. Jaffe, P. V. Doskey, I. McKendry, and T. L. Anderson, Vertical profiles of ozone, aerosols, CO and NMHCs in the Northeast Pacific during the TRACE-P and ACE-Asia experiments, *J. Geophys. Res.*, *108*(D20), 8799, doi:10.1029/2002JD002930, in press, 2003.

Prinn, R. G., J. Huang, R. F. Weiss, D. M. Cunnold, P. J. Fraser, P. G. Simmonds, A. McCulloch, C. Harth, P. Salameh, S. O'Doherty, R. H. J. Wang, L. Porter, and B. R. Miller, Evidence for substantial variation of atmospheric hydroxyl radicals in the past two decades, *Science*, *292*, 1882–1888, 2001.

Raatz, W. E., An anticyclonic point of view on low-level tropospheric long-range transport, *Atmos. Environ.*, *23*, 2501–2504, 1989.

Sander, S. P., et al., Chemical kinetics and photochemical data for use in stratospheric modeling, *JPL Publ. 00-3*, Jet. Propul. Lab., Pasadena, Calif., 2000.

Sander, S. P., et al., Chemical kinetics and photochemical data for use in atmospheric studies, *JPL Publ. 02-25*, Jet Propul. Lab., Pasadena, Calif., 2003.

Schubert, S. D., R. B. Rood, and J. Pfaendtner, An assimilated data set for earth science applications, *Bull. Am. Meteorol. Soc.*, *74*, 2331–2342, 1993.

Snow, J. A., J. B. Dennison, D. A. Jaffe, H. U. Price, J. K. Vaughan, and B. Lamb, Aircraft and surface observations in Puget Sound and a comparison to a regional model, *Atmos. Environ.*, in press, 2003.

Staudt, A. C., D. J. Jacob, J. A. Logan, D. Bachiochi, T. N. Krishnamurti, and G. W. Sachse, Continental sources, transoceanic transport, and inter-hemispheric exchange of carbon monoxide over the Pacific, *J. Geophys. Res.*, *106*, 32,571–32,590, 2001.

Staudt, A. C., D. J. Jacob, F. Ravetta, J. A. Logan, D. Bachiochi, T. N. Krishnamurti, S. T. Sandholm, B. A. Ridley, H. B. Singh, and R. W. Talbot, Sources and chemistry of nitrogen oxides over the tropical Pacific, *J. Geophys. Res.*, *108*(D2), 8239, doi:10.1029/2002JD002139, 2003.

Stohl, A., A 1-year lagrangian climatology of airstreams in the Northern Hemisphere troposphere and lowermost stratosphere, *J. Geophys. Res.*, *106*, 7263–7279, 2001.

Stohl, A., and T. Trickl, A textbook example of long-range transport: Simultaneous observations of ozone maxima of stratospheric and North American origin in the free troposphere over Europe, *J. Geophys. Res.*, *104*, 30,445–30,472, 1999.

Streets, D. G., and S. T. Waldhoff, Present and future emissions of air pollutants in China: SO_2, NO_x, and CO, *Atmos. Environ.*, *34*, 363–374, 2000.

Streets, D. G., et al., An inventory of gaseous and primary aerosol emissions in Asia in the year 2000, *J. Geophys. Res.*, *108*(D21), 8809, doi:10.1029/2002JD003093, in press, 2003.

Thulasiraman, S., N. T. O'Neill, A. Royer, B. N. Holben, D. L. Westphal, and L. J. B. McArthur, Sunphotometric observations of the 2001 Asian dust storm over Canada and the U.S., *Geophys. Res. Lett.*, *29*(8), 1255, doi:10.1029/2001GL014188, 2002.

van Aardenne, J. A., G. R. Carmichael, H. Levy, D. Streets, and L. Hordijk, Anthropogenic NO_x emissions in Asia in the period 1990–2020, *Atmos. Environ.*, *33*, 633–646, 1999.

Wang, Y. H., D. J. Jacob, and J. A. Logan, Global simulation of tropospheric O_3-NO_x-hydrocarbon chemistry: 1. Model formulation, *J. Geophys. Res.*, *103*, 10,713–10,725, 1998.

Wild, O., and H. Akimoto, Intercontinental transport of ozone and its precursors in a three-dimensional global CTM, *J. Geophys. Res.*, *106*, 27,729–27,744, 2001.

World Meteorological Organization (WMO), *Scientific Assessment of Ozone Depletion: 1998*, Geneva, Switzerland, 1999.

Yevich, R., and J. A. Logan, An assessment of biofuel use and burning in agricultural waste in the developing world, *Global Biogeochem. Cycles*, *17*, doi:10.1029/2002GB001952, in press, 2003.

Yienger, J. J., M. Galanter, T. A. Holloway, M. J. Phadnis, S. K. Guttikunda, C. R. Carmichael, W. J. Moxim, and H. Levy II, The episodic nature of air pollution transport from Asia to North America, *J. Geophys. Res.*, *105*, 26,931–26,945, 2000.

Zetzsch, C., and W. Behnke, Heterogeneous photochemical sources of atomic Cl in the troposphere, *Ber. Bunsenges. Phys. Chem.*, *96*, 488–493, 1992.

—————————————

I. Bey, Swiss Federal Institute of Technology, EPFL-ENAC-LMCA, CH-1015 Lausanne, Switzerland. (isabelle.bey@epfl.ch)

M. J. Evans, D. J. Jacob, and P. I. Palmer, Division of Engineering and Applied Sciences, Cambridge, Massachusetts, 02138, USA. (mje@sol.harvard.edu; djj@sol.harvard.edu; pip@sol.harvard.edu)

L. Jaeglé, Department of Atmospheric Sciences, Box 351640, University of Washington, Seattle, Washington, 98195, USA. (jaegle@atmos.washington.edu)

D. A. Jaffe, H. U. Price, and P. Weiss-Penzias, Interdisciplinary Arts and Sciences, University of Washington, 18115 Campus Way, Bothell, Washington, 98011, USA. (djaffe@u.washington.edu; hprice@u.washington.edu; pweiss@bothell.washington.edu)